Numerical detection and continuation of codimension-two homoclinic bifurcations

A.R. Champneys, Yu.A. Kuznetsov

Department of Analysis, Algebra and Geometry

Report AM-R9308 September 1993

CWI is the National Research Institute for Mathematics and Computer Science. CWI is part of the Stichting Mathematisch Centrum (SMC), the Dutch foundation for promotion of mathematics and computer science and their applications.
SMC is sponsored by the Netherlands Organization for Scientific Research (NWO). CWI is a member of ERCIM, the European Research Consortium for Informatics and Mathematics.

P.O. Box 94079, 1090 GB Amsterdam (NL)
Kruislaan 413, 1098 SJ Amsterdam (NL)
Telephone +31 20 592 9333
Telefax +31 20 592 4199

Numerical Detection and Continuation of Codimension-Two Homoclinic Bifurcations

A.R. Champneys*, Yu.A. Kuznetsov†

* *School of Mathematical Sciences,*
University of Bath,
Bath, BA2 7AY, UK
&
Department of Engineering Mathematics, University of Bristol,
Bristol, BS8 1TR, UK

† *Institute of Mathematical Problems of Biology,*
Russian Academy of Sciences, Pushchino, Moscow Region,
142292 Russia
&
CWI,
P.O. Box 94079, 1090 GB Amsterdam, The Netherlands

Abstract

A numerical procedure is presented for the automatic accurate location of certain codimension-two homoclinic singularities along curves of codimension-one homoclinic bifurcations to hyperbolic equilibria in autonomous systems of ordinary differential equations. The procedure also allows for the continuation of multiple-codimension homoclinic orbits in the relevant number of free parameters. All known codimension-two bifurcations that involve a unique homoclinic orbit are considered. In each case the known theoretical results are reviewed and a regular test function is derived. In particular, the test functions for global degeneracies involving the orientation of a homoclinic loop are presented. It is shown how such a procedure can be incorporated into an existing boundary-value method for homoclinic continuation and implemented using the continuation code AUTO. Several examples are studied, including Chua's electronic circuit and the FitzHugh-Nagumo equations. In each case, the method is shown to reproduce codim 2 bifurcation points that have previously been found using *ad hoc* methods, and, in some cases to obtain new results.

AMS Subject Classification (1991): 34C37, 34A50, 58F14
Keywords & Phrases: Homoclinic orbits, global bifurcations, codimension-two bifurcations, continuation method, AUTO
Note: The authors have been supported by a Research Assistantship from the SERC, UK, and by a Visitor grant B 80-61 from the Dutch Science Foundation (NWO), The Netherlands, respectively.

1. Introduction

The aim of the present paper is to develop a robust numerical continuation framework for the analysis of homoclinic bifurcations in parameterized systems of autonomous ordinary differential equations (ODEs). Homoclinic orbits (that is, trajectories which are bi-asymptotic to an equilibrium in such systems) and their associated bifurcations are known to be of importance in a wide number of applications. Examples occur in fields as diverse as mathematical biology, chemistry, fluid mechanics, electronics and probability theory. See, for example, the recent conference proceedings (Gaspard, Arnéodo, Kapral & Sparrow 1993). The existence of homoclinic orbits is typically a *codimension-one* phenomenon (codim 1 for short), that is, one normally has to vary a (single) parameter in the problem in order for them to occur. The problem of interest is then to locate this homoclinic parameter value and, sometimes, to accurately compute the homoclinic orbit there. Such problems typically arise in one of two settings.

Report AM-R9308
ISSN 0924-2953
CWI
P.O. Box 94079, 1090 GB Amsterdam, The Netherlands

The first situation occurs when one studies the dynamics of a model consisting of a system of ODEs. It is then well known that the appearance of an orbit homoclinic to a hyperbolic equilibrium leads, as a generic parameter is varied, to the creation or disappearance of one or more limit cycle (periodic orbit) in an "infinite period" bifurcation. In some cases the bifurcation is of interest as it causes a transition from stable periodic motion to the existence of no stable motion nearby. In other cases, as in the model of Belousov-Zhabotinskii reaction (Arnéodo, Coullet & Tresser (1982), Arniéodo, Argoul, Elezgaray & Richetti (1993)), chaotic trajectories exist in a neighbourhood of the homoclinic bifurcation. In both cases, the phenomenon of interest is not the homoclinic orbit itself, but the organising role it plays for the nearby dynamics. The analysis of homoclinic bifurcations dates back to Andronov & Leontovich (1939) for planar systems, see (Andronov, Leontovich, Gordon & Maier 1971) for a detailed presentation. Then, in a series of papers in late 60's, Shil'nikov (1968, 1970) analyzed homoclinic bifurcations in general n-dimensional systems. It was discovered that, if the equilibrium has complex eigenvalues satisfying certain (open) conditions, there are an infinite number of saddle limit cycles near the original homoclinic orbit for close parameter values. The phenomenon of so called "Shil'nikov chaos" has now became widely known after several modern expositions, notably in Guckenheimer & Holmes (1983). Numerous subsequent publications have improved the original theorems and have established new facts concerning this codim 1 bifurcation, we refer only to Gaspard, Kapral & Nicolis (1984), Glendinning & Sparrow (1984), Tresser (1984), Lin (1990). Many physical applications of Shil'nikov results have also been found; see, for example, (Healey, Broomhead, Cliffe, Jones & Mullin 1991) for an experimental verification.

The second source of interest in homoclinic orbits is that their existence in an system of ODEs can imply the existence of a desired solution of certain partial differential equations (PDEs). The main application here is to *solitary waves* of parabolic and hyperbolic equations (see, for example, surveys by Fife (1978) and Kuznetsov (1982) on travelling waves in reaction-diffusion systems, and the work on water waves by Kirchgassner (1988)), but there are also applications to solutions of certain elliptic problems (Budd 1989). In the former case, one of the parameters in the ODE anzatz is usually the wave speed c. Hence the codim 1 homoclinic orbits in the ODEs correspond to persistent solutions of the PDE and the problem becomes to determine the shape and speed of solitary waves. In contrast to the previous setting, one is thus interested in the homoclinic orbits directly, because the stability of nearby periodic orbits for the ODEs typically has little in common with the stability of periodic waves in the evolution equation. A notable achievement of Shil'nikov's theory in this direction has been the discovery of an infinite number of various travelling impulses and periodic waves in nerve axon equations (Feroe (1981), Evans, Fenichel & Feroe (1982), Kuznetsov & Panfilov (1981)).

Since the appearance of homoclinic orbits corresponds to a global bifurcation, it is usually hard to prove their existence analytically in example systems. The best one can normally hope for is to prove their existence near certain singularities. One way to do this is by locating a codimension-two local bifurcation such as a Bogdanov-Takens or Gavrilov-Guckenheimer point (corresponding to the presence of an equilibrium with eigenvalues $\mu_{1,2} = 0$ or $\mu_1 = 0, \mu_{2,3} = \pm i\omega_0$ respectively) which are the origins of loci of homoclinic orbits in certain cases (Guckenheimer & Holmes 1983, Gaspard 1993). Another way of establishing local existence is by using the so-called Melnikov technique of perturbing certain degenerate, *e.g.* integrable, systems for which the analytic form of a homoclinic orbit is known (see Gruewdler (1992) for some general results using this idea). In other cases, the existence of a homoclinic orbit can be established through some *slow-fast* arguments (see, for example, Jones, Koppel & Langer (1991), Deng (1991), Szmolyan (1991), Kuznetsov, Muratori & Rinaldi (1991)). There are few results concerning the global existence of homoclinic orbits; see (Fiedler 1992) for the first steps in this direction. We do mention, however, that progress has been made recently in global existence for the case of Hamiltonian systems, both using variational methods (*e.g.* Hofer & Wysocki (1990)) and topological methods (*e.g.* Amick & Toland (1992)). Such specialized systems are outside the scope of the present paper. In general then, one has to rely on numerical methods to find homoclinic orbits, to analyze then and to continue their loci in several parameters.

One way to locate a homoclinic orbit numerically is by the continuation of a limit cycle to large period as it approaches a homoclinic orbit (Doedel & Kernévez (1986)). Another technique is to

use shooting, that is, the numerical integration of orbits in the *stable and unstable manifolds* of the equilibrium and the computation of a distance between them (see, for example, Kuznetsov (1983, 1990), Rodríguez-Luis, Freire & Ponce (1990)). Both of these techniques can be extended to facilitate the continuation of homoclinic loci in two parameters. These approaches have obvious limitations and they do not work well in many situations, not least because of numerical instabilities due to the strong divergence of trajectories near hyperbolic equilibria [1] (see, for example, (Sparrow 1982, app. F)). We mention, though, that a form of shooting has recently been used successfully to systematically locate accurate approximations to orbits which are part of an infinite family of homoclinic solutions of systems that have a reversibility property (Champneys & Spence 1993, Champneys & Toland 1993). Such special systems are not considered in the present work.

Boundary-value methods, which are free from the drawbacks mentioned above, have recently been proposed, analyzed and used by Hassard (1980), Miura (1982), Beyn (1990*b*, 1990*a*), Doedel & Friedman (1989) and Friedman & Doedel (1991, 1993, 1993), among others. These methods truncate the homoclinic problem to a finite time interval and impose certain boundary conditions at the end points of that interval. It should be noted that, to date, there is no *standard software* for homoclinic continuation and each research group has its own programs for homoclinic bifurcation analysis which are, at least in some degree, problem specific.

Another drawback of existing research on numerical methods for homoclinic orbit continuation is that there has been no systematic treatment of *codimension-two* homoclinic bifurcations, that is, degeneracies along loci of homoclinic orbits that cause a qualitative change in the nearby dynamics. Let us say more precisely what we mean by a codim 2 homoclinic bifurcation. The nature of a homoclinic bifurcation is known to depend crucially on eigenvalues of the equilibrium and on some global characteristics of the phase portrait near the homoclinic orbit at the bifurcation parameter values (like the *twistedness* of the stable and unstable manifolds around the homoclinic orbit). These topological characteristics are important since, for example, they determine the direction of the limit cycle bifurcation under parameter variation. More generally, a particular bifurcation scenario near the homoclinic bifurcation is determined by some (local and global) *non-degeneracy conditions*. If one of these conditions is violated, a *codimension two* homoclinic bifurcation may appear. If a homoclinic bifurcation is traced in two parameters, such bifurcations appear at isolated points on the homoclinic locus (curve). Finding such a point allows one to predict a change in the bifurcation scenario caused by the homoclinic orbit. Typically there are are loci of (sometimes infinitely many) different bifurcation curves in a neighbourhood of the codim 2 point on the parameter plane. Many such codim 2 homoclinic bifurcations have recently been analyzed theoretically (see the references in sec. 2) and some have proved to be important in applications.

Let us mention three recent examples of codim 2 homoclinic bifurcations which highlight their importance. In each case, the phenomenon of interest is the existence of chaos in the neighbourhood of a homoclinic orbit and there is a Bogdanov-Takens point from which a homoclinic orbit emanates. [2] The first system is Chua's electronic oscillator (Khibnik, Roose & Chua (1993), see also Healey et al. (1991), Freire, Rodríguez-Luis & Ponce (1993) and secs. 5.4, 5.5 below) where the eigenvalues of the equilibrium become complex along the homoclinic locus and then satisfy the conditions for Shil'nikov chaos. In the second system, the Shimizu-Morioka equation (Rucklidge (1993), Shil'nikov (1993), see also sec. 5.5 below), there is a transition along the homoclinic locus to a pair of homoclinic orbits satisfying the same conditions as in the Lorenz equations (Lorenz 1963, Sparrow 1982) and then a further transition caused by a change in the relative magnitude of the two eigenvalues closest to zero. The final system is the model of articulated pipes considered in (Champneys 1993) where the global twistedness of the unstable manifold changes in an *inclination switch* bifurcation (see sec. 2 below for a precise definition). In each of the three cases a "horn" of parameter values emanates from the particular codim 2 homoclinic orbit, inside which there are chaotic dynamics. These codim 2 points

[1] This divergence typically prevents one from finding good approximations to homoclinic solutions but can provide accurate estimates to homoclinic parameter values.

[2] In fact, each of the three systems has a form of $\mathbb{Z}_2$- symmetry, which implies that there are three periodic orbits in a neighbourhood of a symmetry-related pair of homoclinic orbits. This symmetry aspect is unimportant for the present discussion.

can thus be thought of as the "organizing centers" for the interesting dynamics.

The need is therefore paramount for a systematic approach to analyze homoclinic bifurcations during numerical continuation and to detect such codim 2 points. Our goal in the present paper is satisfy this need. In so doing we hope to bridge some gaps between pure and applied homoclinic bifurcation theory by highlighting to the applied community these codim 2 phenomena, which we believe have already proved to be fundamental to the understanding of complicated dynamics in examples. We also wish to supply the practitioner with a computational framework within which to locate these phenomena in new, as yet unstudied, examples.

The paper is organized as follows. In sec. 2 we formulate non-degeneracy conditions determining codim 1 homoclinic bifurcations and formulate the famous theorems by Shil'nikov. We then classify certain degenerate, *i.e.* codim 2, cases and give a brief description of what is known from the available literature on the structure of parametric portraits near each bifurcation. We do not touch *local* bifurcations involving homoclinic orbits or *heteroclinic* bifurcations (when a cycle is formed by several orbits connecting equilibria or other invariant sets), nor bifurcations associated with the presence of several orbits homoclinic to the same equilibrium. Section 3 is devoted to a detailed description of a boundary-value approach for the continuation of the homoclinic orbit in two parameters, which follows Beyn (1990*b*). Some possible variants of the same approach are also discussed and evaluated. In sec. 4 we propose *test functions* to detect, along codim1 homoclinic loci, each of the codim 2 bifurcations we study. The functions for the detection of global singularities, (*inclination* and *orbit switches*), seem to be new. In the last section we describe an implementation of the proposed algorithm as a standard *driver*[3] to AUTO, a well known continuation software by Doedel & Kernévez (1986). Methods of obtaining starting solutions for continuation are discussed within this setting. Then we present numerical results on four example systems (the FitzHugh-Nagumo wave system, Chua's electronic circuit, a similar electronic circuit model by Friere *et al.* and the Shimizu-Morioka equations). The presence of codim 2 homoclinic bifurcations are known for these systems, and we use them mainly as "test problems". However, some of the features we present are new; notably a codim 3 homoclinic bifurcation occurring in Chua's circuit and a non-transversal codim 2 homoclinic bifurcation in the FitzHugh-Nagumo equations.

Acknowledgements: The authors thankfully acknowledge helpful discussions with E.Doedel (Caltech, Pasadena/Concordia University of Montreal) and B.Sandstede (Institute fur Angewandte Analysis und Stochastik, Berlin), the latter of whom first suggested to us the use of adjoint variational equations. Several theoretical questions have been clarified for us by L.Shil'nikov, L.Belyakov (Institute of Applied Mathematics and Cybernetics, Nizhnii Novgorod) and Bo Deng (University of Nebraska, Lincoln) through personal communications. ARC has been supported by a research assistantship from the SERC, UK, and YuAK by visitor grant B 80-61 from the Dutch Science Foundation (NWO), The Netherlands.

2. Homoclinic Orbits

2.1 Non-degenerate Homoclinic Orbits

Throughout this paper we shall consider sufficiently smooth, generic dynamical systems of the form

$$\dot{x} = f(x,\alpha), \quad x \in \mathbb{R}^n,\ \alpha \in \mathbb{R}^p. \tag{2.1}$$

Suppose that at some parameter value $\alpha = 0$, say, there is an orbit Γ of (2.1) that is homoclinic to an equilibrium. Without loss of generality, take the equilibrium to be O, the origin of $\mathbb{R}^n$. That is,

$$\Gamma = \{\gamma(t) \mid t \in \mathbb{R}\}, \quad \text{where} \quad \lim_{t\to\pm\infty} \gamma(t) = 0.$$

We assume that

($H.0$) Γ *is the only orbit homoclinic to* O *at* $\alpha = 0$.

[3]The driver program is available from the first author on request.

Let $A = (D_x f)(0,0)$. Suppose that A has n_s eigenvalues μ_i, $i = 1, \ldots, n_s$, with non-positive real part and n_u eigenvalues λ_i, $i = 1, \ldots, n_u$, with positive real part (counting multiplicities), such that

$$n_u + n_s = n,$$

$$\mathrm{Re}\{\mu_{n_s}\} \leq \ldots \leq \mathrm{Re}\{\mu_2\} \leq \mathrm{Re}\{\mu_1\} \leq 0 < \mathrm{Re}\{\lambda_1\} \leq \mathrm{Re}\{\lambda_2\} \ldots \leq \mathrm{Re}\{\lambda_{n_u}\}.$$

Assume that

(H.1) *the equilibrium is hyperbolic*: $\mathrm{Re}\{\mu_1\} \neq 0$.

It follows from (H.1) that there are no other equilibria in a neighbourhood of O.

Stable and unstable manifolds $W^{s,u}(O)$ of O are defined by

$$\begin{aligned} W^s(O) &= \{x \in \mathbb{R}^n \mid \varphi^t(x) \to 0 \text{ as } t \to +\infty\}, \\ W^u(O) &= \{x \in \mathbb{R}^n \mid \varphi^t(x) \to 0 \text{ as } t \to +\infty\}, \end{aligned}$$

where φ^t is the flow corresponding to (2.1). The only stable and unstable manifolds of interest in the sequel will be those of O, hence $W^{u,s}$ shall be used as a shorthand notation for $W^{u,s}(O)$. Under the assumption (H.1), it is well known that $W^{u,s}$ are immersed sub-manifolds of $\mathbb{R}^n$ of dimension n_u and n_s respectively which are tangent at O to the stable and unstable eigenspaces of A (Guckenheimer & Holmes 1983). At each point $\gamma(t) \in \Gamma$ two tangent spaces are defined:

$$X(t) = T_{\gamma(t)} W^s, \; Y(t) = T_{\gamma(t)} W^u.$$

Let $Z(t) = X(t) + Y(t)$ and notice that $\dim Z(t) < n$ since the vector $\dot{\gamma}(t) \in X(t) \cap Y(t)$. We assume the following non-degeneracy condition

(H.2) $$\mathrm{codim}\; Z(t) = 1,$$

that is, $X(t) \cap Y(t) = \mathrm{span}\{\dot{\gamma}(t)\}$. The condition ($H$.2) can also be expressed analytically as follows. Let $B(t) = (D_x f)(\gamma(t), 0)$. Then ($H$.2) means that, to within a scalar multiple, $y(t) = \dot{\gamma}(t)$ is the unique bounded solution of the *variational equation* around the homoclinic orbit:

$$\dot{y} = B(t)y, \; y \in \mathbb{R}^n. \tag{2.2}$$

All eigenvalues μ_i such that $\mathrm{Re}\{\mu_i\} = \mathrm{Re}\{\mu_1\}$ are termed *leading (principle) stable* eigenvalues, and, similarly, the eigenvalues in the right half of the complex plane whose real parts are closest to the imaginary axis are termed *leading (principle) unstable* eigenvalues. The corresponding (generalised) eigenvectors and eigenspaces are also called leading. If all the leading eigenvalues are real, the origin is said to be a *real saddle* (*saddle*, for short); if all the leading eigenvalues are complex the origin is termed *focus-focus (bi-focus)*. In all other cases it is called a *saddle-focus*. Clearly, since A is a real matrix, complex eigenvalues (*i.e.* not real) must occur in complex conjugate pairs. Therefore, in the case of a saddle-focus or focus-focus at least one of the leading eigenspaces must be multi-dimensional. Among all (stable and unstable) leading eigenvalues, those which are closest to the imaginary axis will be called *determining* in the following. Suppose

(H.3) *the leading eigenspaces are either one- or two-dimensional.*

Moreover, let the following non-degeneracy conditions for the leading eigenvalues hold:

(H.4) $$\mu_1 \neq -\lambda_1, \quad \text{with} \quad \mathrm{Im}\{\mu_1\} = \mathrm{Im}\{\lambda_1\} = 0;$$

(H.5) $$\mu_1 \neq \mu_2, \quad \text{with} \quad \mathrm{Im}\{\mu_1\} = \mathrm{Im}\{\mu_2\} = 0;$$

(H.6) $$\mathrm{Re}\{\mu_1\} \neq -\mathrm{Re}\{\lambda_1\}, \quad \text{with} \quad \mathrm{Im}\{\mu_1\} \neq 0;$$

$$(H.7) \qquad \mathrm{Re}\{\mu_1\} \neq -\frac{1}{2}\lambda_1, \quad \text{with} \quad \mathrm{Im}\{\mu_1\} \neq 0, \mathrm{Im}\{\lambda_1\} = 0;$$

as well as the corresponding inequalities obtained by reversing time (i.e. replacing μ_i by λ_i).

Following Shil'nikov (1968) (see Hirsch, Pugh & Shub (1977) for proofs), one can define the *non-leading stable manifold* W^{ss} (*non-leading unstable manifold* W^{uu}) to be the invariant sub-manifold of W^s (respectively W^u) that is tangent at the origin to the non-leading stable (unstable) eigenspace. Let $p, q, \in \Gamma$ be points sufficiently close to O; $p \in W^u_{\mathrm{loc}}$, $q \in W^s_{\mathrm{loc}}$, where $W^{u,s}_{\mathrm{loc}}$ are local unstable and stable manifolds of O defined with respect to sufficiently small neighbourhood of O. We assume that, at $\alpha = 0$,

$$(H.8) \qquad p \notin W^{uu},$$

$$(H.9) \qquad q \notin W^{ss},$$

which implies that the homoclinic orbit is tangent at the origin to the leading eigenspaces. For example, in the saddle case, let

$$e(t) = \frac{\dot{\gamma}(t)}{\|\dot{\gamma}(t)\|} \quad \text{and} \quad e^{\pm} = \pm \lim_{t \to \mp\infty} e(t),$$

then e^+ is a unit eigenvector corresponding to λ_1 and e^- is a unit vector corresponding to μ_1. Finally, suppose that in the saddle case the homoclinic orbit satisfies the *strong inclination properties* (Shil'nikov 1968, Deng 1989). That is

$$(H.10) \qquad \lim_{t \to -\infty} Z(t) = T_O W^{ss} \oplus T_O W^u,$$

$$(H.11). \qquad \lim_{t \to +\infty} Z(t) = T_O W^{uu} \oplus T_O W^s,$$

Note, due to $(H.2)$, that $Z(t)$ divides $\mathbb{R}^n$ for each t. A saddle homoclinic orbit satisfying $(H.10)$ and

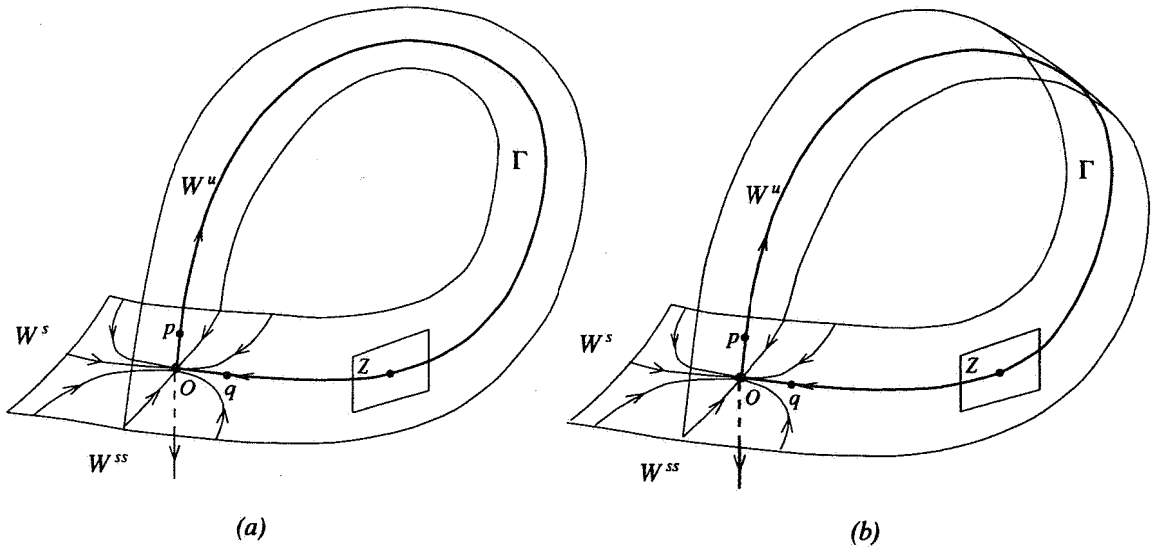

Figure 2.1: Non-twisted *(a)* and twisted *(b)* saddle homoclinic orbits in $\mathbb{R}^3$.

$(H.11)$ is said to be *twisted* if e^- and e^+ point to the opposite sides of $Z(t)$ at p and q respectively. Otherwise, it is *non-twisted*. See fig. 2.1.

Definition 2.1 *A homoclinic orbit is called* regular *if assumptions* $(H.0)$-$(H.2)$ *hold.*

Definition 2.2 *A regular orbit that is homoclinic to a saddle-focus or focus-focus is called* non-degenerate *if assumptions* $(H.3)$-$(H.9)$ *hold, while a regular orbit that is homoclinic to a saddle is called non-degenerate if* $(H.3)$-$(H.11)$ *hold.*

For a system (2.1) depending generically upon parameters, those parameter values which correspond to the presence of a regular homoclinic orbit form a smooth sub-manifold $\mathcal{H}$ of codimension one in the parameter space $\mathbb{R}^p$ of the system. This manifold is a regular zero level surface of a smooth function (the *Melnikov functional*) measuring the distance between $W^u(O)$ and $W^s(O)$. The manifold $\mathcal{H}$ is partitioned into several regions $\mathcal{H}_i$ corresponding to different non-degenerate sub-cases. Violation of any of the non-degeneracy assumptions defines a codimension-two boundary of $\mathcal{H}_i$. It is known (mainly due to L.P.Shil'nikov) that a transversal crossing of an $\mathcal{H}_i$ implies a particular bifurcation scenario for the phase portrait near the homoclinic orbit.

Theorem 2.1 (Shil'nikov (1968),"tame homoclinic bifurcation") *If parameters are varied in a generic system* (2.1) *such that a sub-manifold is crossed corresponding to a non-degenerate saddle homoclinic orbit or a saddle-focus homoclinic orbit with a real determining eigenvalue then a unique periodic orbit bifurcates from the homoclinic orbit. The period of the orbit tends to infinity as the bifurcation is approached.*

Theorem 2.2 (Shil'nikov (1970),"chaotic homoclinic bifurcation") *An infinite number of periodic orbits with arbitrarily high periods exist in a neighbourhood of the homoclinic orbit of a generic system* (2.1) *for parameter values near a sub-manifold corresponding to a non-degenerate focus-focus or saddle-focus homoclinic orbit with complex determining eigenvalues.*

In the latter case, loosely speaking, there is an infinite number of Smale horseshoes (Smale 1967) at the critical parameter value and a finite number of them for nearby parameter values. As $\mathcal{H}_i$ is crossed, the horseshoes are successively created or destroyed. The crossing of the homoclinic manifold implies an infinite number of fold and flip (period-doubling) bifurcations involving the periodic orbits. Therefore, for example, there is an infinite series of codim 1 manifolds $\{\mathcal{S}_k^{(2)}\}$ of fold bifurcations which accumulate (from the both sides) on $\mathcal{H}_i$ as $k \to \infty$. Also, there is a one-sided sequence of codim-1 manifolds $\{\mathcal{H}_j^{(2)}\}$ which accumulates on $\mathcal{H}_i$ as $j \to \infty$, each corresponding to the existence of a *double* homoclinic orbit (that is, an orbit that makes two "big" excursions near the primary homoclinic orbit before returning to the equilibrium) (Evans et al. 1982, Gaspard 1983, Feroe 1986, Glendinning 1989*b*).

Notice that it can not be said that two generic one-parameter systems crossing the same $\mathcal{H}_i$ are always locally topologically equivalent in a neighbourhood of the homoclinic orbit, even if there is only one periodic orbit present near the bifurcation. A relevant counter-example is provided by a saddle-focus homoclinic orbit with a real determining eigenvalue. Actually, it is proved that for systems with a saddle-focus homoclinic orbit the ratio

$$\nu = -\frac{\lambda_1}{\mathrm{Re}\{\mu_{1,2}\}}$$

is a *topological invariant*, provided that $\mu_{1,2}$ are complex while λ_1 is real (Afraimovich, Arnold, Il'yashenko & Šil'nikov 1993). Therefore, the sub-manifold $\mathcal{H}_i$ corresponding to the saddle-focus homoclinic orbit is foliated by codimension-two sub-manifolds $\{\nu = const\}$ on any two of which the phase portraits near the homoclinic orbit are non-equivalent. This prevents the existence of a "universal unfolding" for the homoclinic bifurcation in which a saddle-focus is involved.

We shall see later on, that not all *formal* boundaries of $\mathcal{H}_i$ given by violation of a non-degeneracy condition do correspond to the presence of topologically distinct phase portraits near $\mathcal{H}$.

2.2 The Degenerate Cases

There now follows a brief description of what is known from the existing literature about the dynamics in a neighbourhood of each of the codimension-two points arising through the violation of an assumption from $(H.0)$-$(H.11)$. It must be pointed out that the corresponding codimension-two bifurcations

have been studied with differing degrees of detail. Some of the cases are treated only for systems in the lowest possible dimensions while others, to our knowledge, have received no attention as yet. Earlier attempts to survey some of the codim 2 homoclinic bifurcations can be found in (Kuznetsov 1983, Glendinning 1988, Belyakov & Shil'nikov 1990, Fiedler 1992).

Suppose that our system depends generically on two parameters $\alpha = (\alpha_1, \alpha_2)$. Then the homoclinic manifold is a curve $\mathcal{H}^{(1)}$. While moving along this curve, one of the assumptions $(H.0)$-$(H.11)$ can be violated at some point. In the following we describe the parametric portrait of such a generic system in the (α_1, α_2)-plane near the codimension-two bifurcation point which we suppose, for simplicity, occurs at $\alpha = 0$. Moreover, we assume that the parameters are selected in such a way that the "primary" homoclinic branch $\mathcal{H}^{(1)}$ is locally defined by the axis $\{\alpha_2 = 0\}$.

Neutral (resonant) saddle Suppose that the equilibrium is a saddle and that all the non-degeneracy assumptions except $(H.4)$ hold, that is the leading eigenvalues are real and simple but

$$\mu_1 = -\lambda_1. \tag{2.3}$$

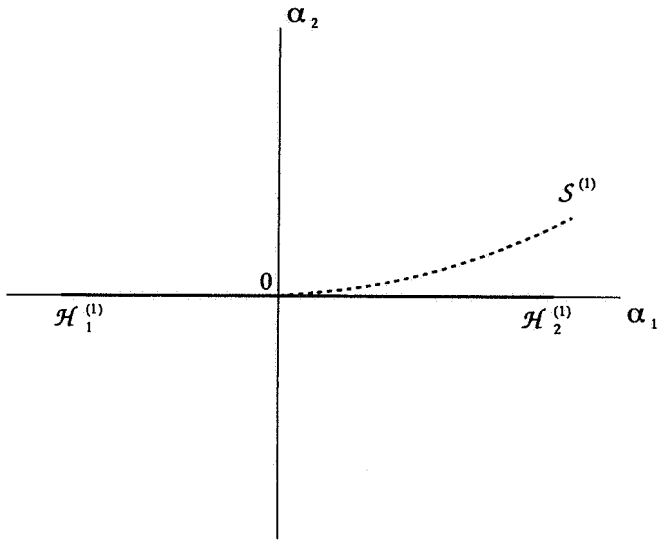

Figure 2.2: Resonant side-switching.

This case was studied completely by Nozdrachova (1982) for two-dimensional systems and by Chow, Deng & Fiedler (1990) in the n-dimensional situation. There are two sub-cases depending on the twistedness of the homoclinic orbit.

If the homoclinic orbit is non-twisted, we have the so called *resonant side-switching* bifurcation. The codim 2 bifurcation point is the source of an extra codimension-one bifurcation curve $\mathcal{S}^{(1)}$ corresponding to a fold (saddle-node) bifurcation of periodic orbits. Two limit cycles of different stability, which appear while crossing the homoclinic bifurcation branches $\mathcal{H}^{(1)}_{1,2}$ separated by the codim 2 point, collide and disappear on this extra curve (see fig. 2.2).

If the homoclinic orbit is twisted, then so called *resonant homoclinic doubling* takes place. Two different curves originate at the critical point, namely a curve $\mathcal{H}^{(2)}$ corresponding to the appearance of a double homoclinic orbit (see fig. 2.3), and a curve $\mathcal{F}$ at which an orbit of "double" period appears through a period-doubling bifurcation (fig. 2.4). It is proved in Kisaka, Kokubu & Oka (1993*a*) that secondary homoclinic orbits which make more than two large excursions do not bifurcate in this case.

Double real leading eigenvalue Assume that the equilibrium under investigation is a saddle with a homoclinic orbit for which all the conditions but $(H.5)$ hold:

$$\mu_1 = \mu_2. \tag{2.4}$$

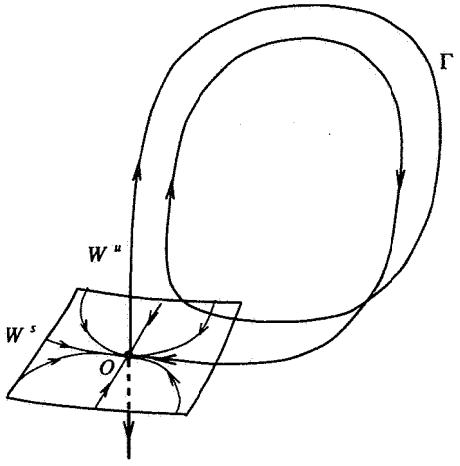

Figure 2.3: A double homoclinic orbit to a saddle.

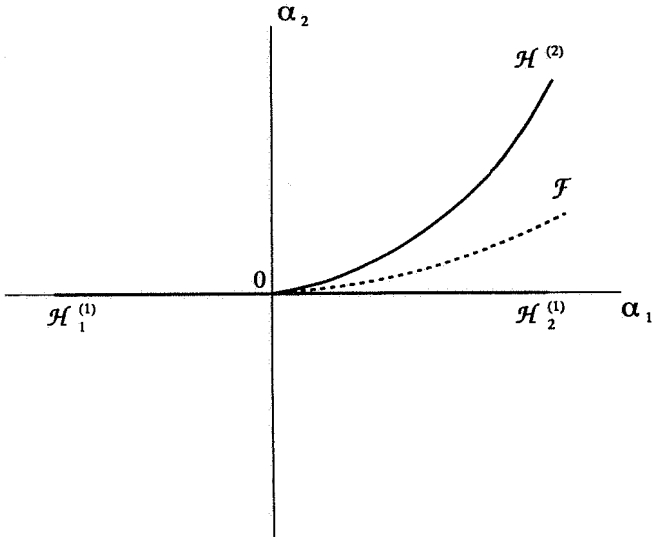

Figure 2.4: Resonant homoclinic doubling.

Typically, this degeneracy causes a transition from a saddle to a saddle-focus (or from saddle-focus to focus-focus) while moving along the homoclinic curve. A codim 2 bifurcation appears when this double leading eigenvalue is determining, because the codim 1 homoclinic bifurcation switches from tame to chaotic upon crossing the codim 2 point along the homoclinic curve. If the double eigenvalues are not determining then the homoclinic bifurcation remains tame and the parametric portrait contains no bifurcation curves at which limit cycles can bifurcate other than that of the primary homoclinic branch. The former case has been studied by Belyakov (1980) for three-dimensional systems. There are two bundles each consisting of an infinite number of bifurcations curves: $\{\mathcal{H}_j^{(2)}\}_{j=1}^{\infty}$ corresponding to double homoclinic orbits making different (increasing) numbers of "rotations" near the saddle-focus during their first return (*i.e.* between the two large excursions), and $\{\mathcal{S}_j^{(1)}\}_{j=1}^{\infty}$ corresponding to fold bifurcations of periodic orbits with different numbers of small rotations (see fig. 2.5). The bundles extend from the origin into the saddle-focus region and the double homoclinic curves occur on only one side of the primary homoclinic bifurcation curve. The relative position of $\{\mathcal{H}_j^{(2)}\}_{j=1}^{\infty}$ with respect to $\mathcal{H}^{(1)}$ is determined by the twistedness of the saddle homoclinic orbit along $\mathcal{H}_1^{(1)}$, or, equivalently, by the direction of a cycle bifurcation while crossing this curve. It should be noted that

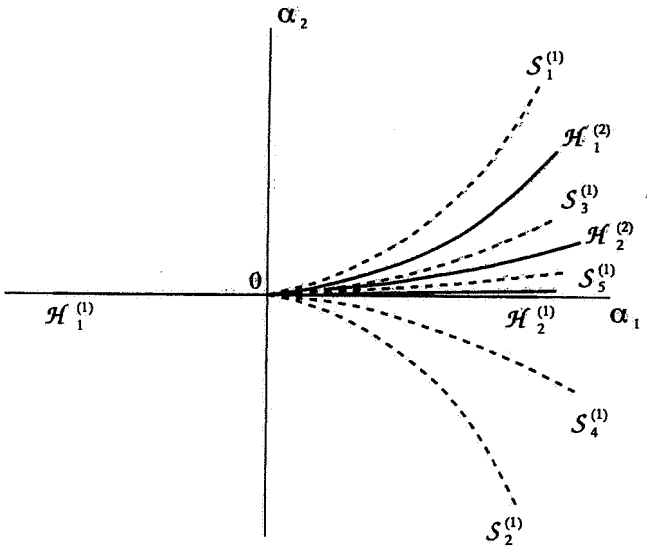

Figure 2.5: Double eigenvalue.

the number of rotations near the saddle-focus also increases when the parameters approach the origin along each double homoclinic or fold bifurcation curve. The complete bifurcation structure for this case is unknown, and it seems reasonable to expect also an infinite series of period-doubling bifurcation curves originating at (or accumulating on) O.

Neutral (resonant) saddle-focus Suppose that the equilibrium is a saddle-focus and that all the non-degeneracy assumptions except (H.6) are satisfied, that is

$$\mathrm{Re}\{\mu_1\} = -\mathrm{Re}\{\lambda_1\}. \tag{2.5}$$

If one of the leading eigenspaces is one-dimensional then, generically, there is a transition from a tame to a chaotic homoclinic bifurcation due to the determining eigenspace changing from a real eigenspace to a complex one. Only the three-dimensional case seems to have been studied. The complete picture is unknown, but the following results are due to Belyakov (1984). Generically, there are several infinite series of codim 1 bifurcation curves that accumulate in a complex manner on the origin of the (α_1, α_2)-plane. More precisely, there is a countable number of curves $\{S_j^{(1)}\}_{j=1}^{\infty}$ corresponding to fold bifurcations of cycles with increasing number of rotations near the saddle-focus. Each of the curves has a codim 2 singularity of *cusp* type. The cusp points $\mathcal{C}_j$ accumulate on the origin (see fig. 2.6). The other infinite series of codim 1 bifurcation curves is composed of double homoclinic curves $\{\mathcal{H}_k^{(2)}\}_{k=1}^{\infty}$ all of which have horizontal asymptotes and have extremum points which accumulate at $\alpha = 0$. These curves are all located to one side of the primary homoclinic curve (this side is determined by the direction of bifurcation of the unique cycle upon crossing the part $\mathcal{H}_1^{(1)}$ of the homoclinic curve corresponding to the saddle-focus with a real determining eigenvalue). The whole picture is even more involved, since there is a countable set of various *triple* homoclinic bifurcation curves $\{\mathcal{H}_{km}^{(3)}\}_{k,m=1}^{\infty}$ located between *each* pair of double homoclinic curves $\mathcal{H}_k^{(2)}$ and $\mathcal{H}_{k+1}^{(2)}$. Only a few of them are shown in fig. 2.6.

Neutrally-divergent saddle-focus This singularity means that the sum of all leading eigenvalues of a saddle-focus with a one-dimensional leading eigenspace is zero (condition (H.7) is violated):

$$\mathrm{Re}\{\mu_1\} = -\frac{1}{2}\lambda_1, \tag{2.6}$$

with real λ_1. In the three-dimensional case this means that the divergence of the vector field (2.1) vanishes at O. The bifurcation implies a transition from the presence of *stable* limit cycles with arbitrarily high period near the primary homoclinic bifurcation to the presence of long-period *totally*

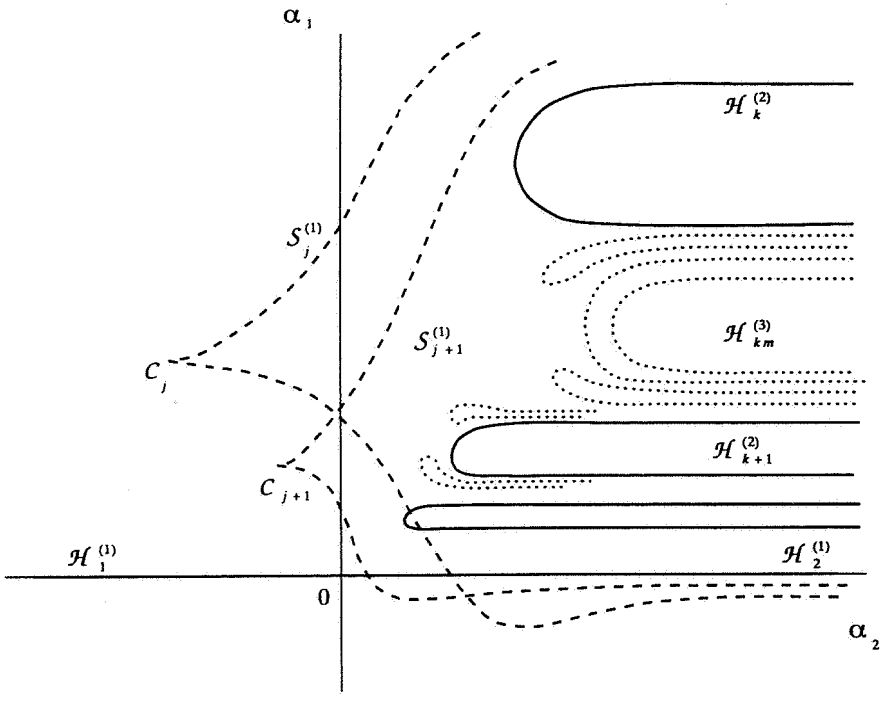

Figure 2.6: Resonant saddle-focus.

unstable ones (Gaspard 1983, Glendinning & Sparrow 1984). The complete bifurcation picture is, once again, unknown.

Three leading eigenvalues Suppose that $(H.3)$ does not hold and that the determining eigenspace is *three-dimensional* due to the presence of a simple real eigenvalue and a simple complex pair of eigenvalues with the same real part:

$$\mathrm{Re}\{\mu_1\} = \mathrm{Re}\{\mu_2\} = \mu_3. \tag{2.7}$$

This case implies a change of the dimension of the determining eigenspace while moving along the primary homoclinic curve. When the determining eigenspace is one-dimensional the homoclinic bifurcation is tame and when this eigenspace is two-dimensional the homoclinic bifurcation is chaotic. This, then, is another example of a tame-to-chaotic transition, but, unlike the previous two cases (subsecs. 2.2.2, 2.2.3), nothing definite seems to be known about the two-parameter picture in this situation.

In all the previous cases the equilibrium remained hyperbolic. The following two cases involve non-hyperbolic equilibria having a homoclinic orbit which can be approached by following a non-degenerate homoclinic orbit. Note that there are other types of orbits homoclinic to a non-hyperbolic equilibria which can not be approached as the limit of a non-degenerate homoclinic orbit (see, for example (Shil'nikov 1969) and sect. 2.2.6 below).

Saddle-node homoclinic orbit While moving along a homoclinic bifurcation curve corresponding to a saddle homoclinic orbit, another equilibrium can approach the one to which the primary homoclinic orbit occurs. At the critical parameter values, there is a non-hyperbolic equilibrium, *i.e.* $(H.1)$ does not hold, with

$$\mu_1 = 0, \tag{2.8}$$

and a homoclinic orbit leaving it along the unstable manifold and returning along the center manifold (see, fig. 2.7). This case has been studied by a number of authors, first by Lukyanov (1982) for planar

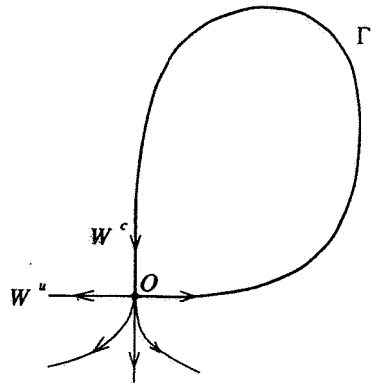

Figure 2.7: Saddle-node homoclinic orbit.

systems and by Chow & Lin (1990) and Deng (1990) in general. The parametric portrait is shown in fig. 2.8. Here there is a curve s of fold bifurcations of the equilibria and a primary homoclinic

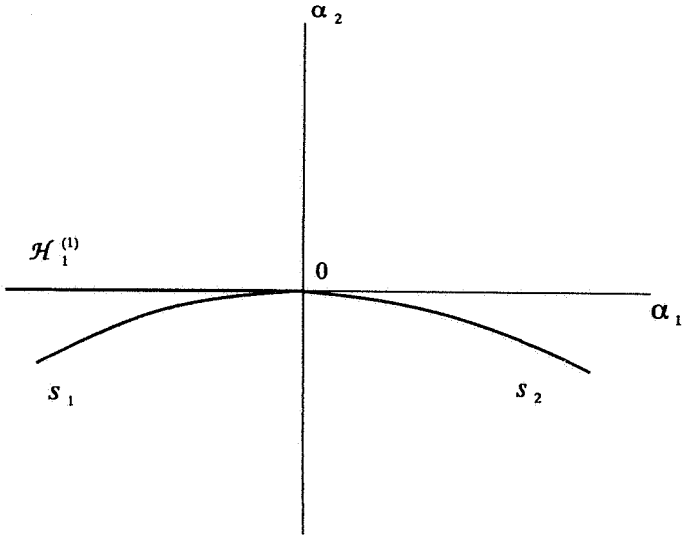

Figure 2.8: Saddle-node homoclinic bifurcation portrait.

bifurcation curve $\mathcal{H}_1^{(1)}$ which terminates at the origin. The codim 2 point is thus an *end point* of the curve of homoclinic orbits to hyperbolic equilibria. However, along the part s_2 of the fold curve (which is a "continuation" of $\mathcal{H}_1^{(1)}$), there is a homoclinic orbit to the non-hyperbolic equilibrium that is tangent as $t \to \pm\infty$ to the central eigenspace. Despite being degenerate according to Definition 2.1, such a homoclinic orbit is of codimension one.

Shil'nikov-Hopf While moving along a homoclinic bifurcation curve corresponding to a saddle-focus, the equilibrium can undergo a Hopf bifurcation at certain parameter values. This is another way to violate $(H.1)$:

$$\mathrm{Re}\{\mu_{1,2}\} = 0. \tag{2.9}$$

This codim 2 case has been analysed by Belyakov (1974) and by Gaspard (1987) and Hirshcberg & Knobloch (1993) all in three-dimensions with the Hopf bifurcation being supercritical. The homoclinic curve $\mathcal{H}_1^{(1)}$ terminates at the codim 2 point having a non-zero angle with the Hopf bifurcation curve h passing through the origin (see fig. 2.9). On a continuation of $\mathcal{H}_1^{(1)}$ to the other side of h there is a

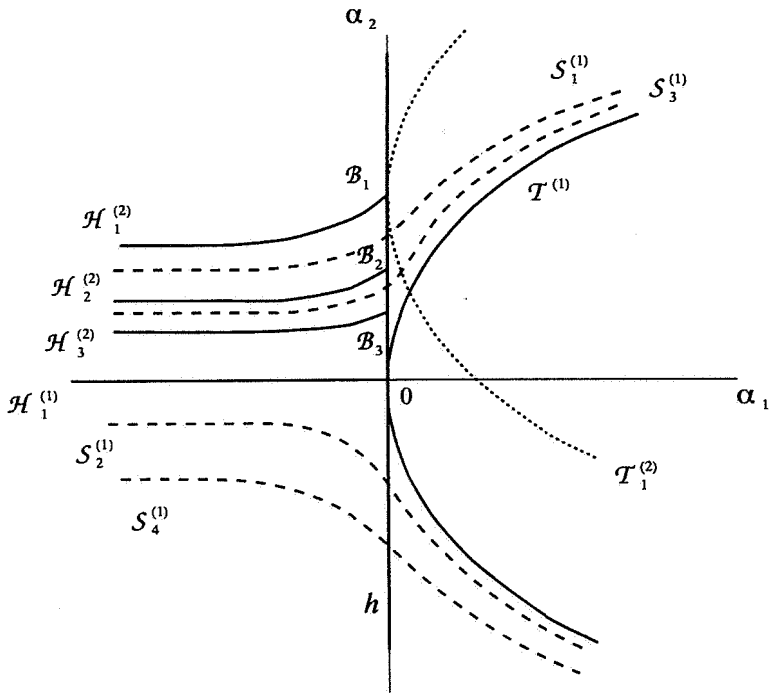

Figure 2.9: Shil'nikov-Hopf.

point-to-periodic heteroclinic orbit, that is, an orbit which connects the non-leading unstable manifold of O to the stable manifold of the cycle C that appears through the Hopf bifurcation on h. A parabola-like curve $\mathcal{T}^{(1)}$ corresponds to a tangency between the two-dimensional stable and unstable invariant manifolds of C *i.e.* there is a *non-transversal homoclinic orbit to a cycle*). Bifurcation sequences associated with a non-transversal homoclinic orbit to a cycle have been analysed by Gavrilov & Silnikov (1972, 1973) and Gaspard & Wang (1987). Inside the parabola, a transversal homoclinic structure associated with the cycle is present. There are two infinite series of other codim 1 bifurcation curves: $\{\mathcal{H}_j^{(2)}\}_{j=1}^{\infty}$ accumulating on the primary homoclinic curve $\mathcal{H}_1^{(1)}$, each of them having a termination point $\mathcal{B}_k$ at the Hopf curve; and $\{\mathcal{S}_k^{(1)}\}_{k=1}^{\infty}$ accumulating (from both sides) on the union $\mathcal{H}_1^{(1)} \cup \mathcal{T}^{(1)}$. Each point $\mathcal{B}_k$ is the vertex of another "parabola" $\mathcal{T}_k^{(2)}$ corresponding to a tangency between stable and unstable invariant manifolds of C along a homoclinic orbit making *two* big excursions around the primary homoclinic one (a *double* non-transversal homoclinic orbit to a cycle). The complete picture is unknown.

The final two cases we consider are caused by certain global degeneracies of saddle homoclinic orbits and are therefore undetectable by monitoring the eigenvalues.

Orbit switch (non-leading homoclinic orbit to a saddle) This case occurs when one of the assumptions $(H.8)$ or $(H.9)$ is violated, that is, the homoclinic orbit tends to the saddle (in one time direction) along its *non-leading* eigenvector (fig. 2.10). Notice that the twist type of the homoclinic orbit *changes* at this bifurcation point. This case has recently been studied by Sandstede (1993). Suppose the system (2.1) is three-dimensional and let $\mu_2 < \mu_1 < 0 < \lambda_1$. There are several different parametric portraits depending on the further relative positions of the eigenvalues.

If $\lambda_1 < |\mu_1|$, then the parametric portrait of the system contains no bifurcation curves except the primary homoclinic branch. At most one saddle cycle is present near the bifurcation. Thus, this codim 2 bifurcation is somehow trivial.

If $|\mu_1| < \lambda_1 < |\mu_2|$, then the parametric portrait of the system near the bifurcation is as presented in fig. 2.11. There are three extra curves originating at the critical point on the primary homoclinic

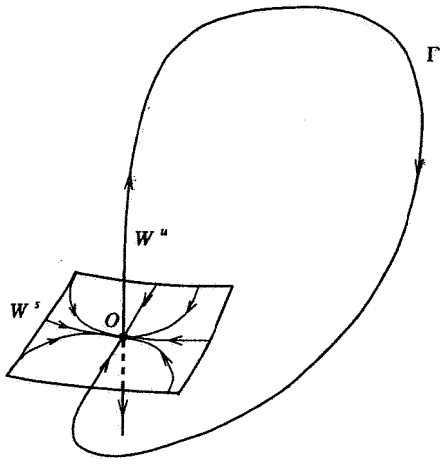

Figure 2.10: Non-leading homoclinic orbit.

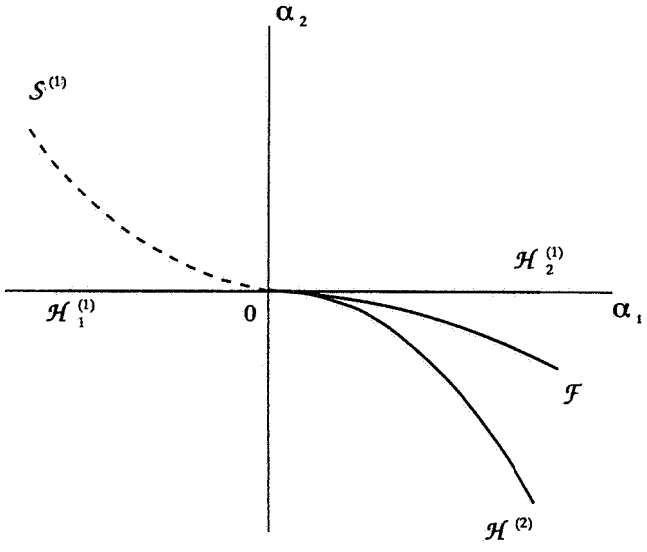

Figure 2.11: Orientation homoclinic doubling.

curve: $\mathcal{S}^{(1)}$ corresponding to a fold bifurcation of the periodic orbits that are generated by the primary homoclinic bifurcation; $\mathcal{F}$ corresponding to a period-doubling bifurcation of one of these cycles; and a double homoclinic curve $\mathcal{H}^{(2)}$. There are more other periodic orbits nearby and no other bifurcation curves originating at the critical point. This case is thus similar to resonant homoclinic doubling, as first pointed out by Yanagida (1987), and we call it *orientation homoclinic doubling.*

If $|\mu_1| < |\mu_2| < \lambda_1$, then the parametric portrait includes curves $\mathcal{S}^{(1)}$ and $\mathcal{F}$ defined above and an *infinite* series of secondary homoclinic bifurcation curves $\{\mathcal{H}^{(j)}\}_{j=2}^{\infty}$ originating at the codim 2 point (see fig. 2.12). The later series accumulates on the primary homoclinic orbit curve either from the same side as $\mathcal{S}^{(1)}$ and $\mathcal{F}$ or the other (only one case is shown in the figure). There is also a region (not shown in the figure) in which the dynamics of the system contains Smale horseshoes. Note that, while the homoclinic bifurcation along $\mathcal{H}_2^{(1)}$ remains tame in the sense of Thm. 2.1, chaotic dynamics exist near the primary homoclinic curve for $\alpha_2 > 0$. We refer to this phenomenon as *orientation homoclinic splitting.* The complete picture is unknown.

Inclination switch (neutrally-twisted homoclinic orbit to a saddle) The last codim 2 bifurcation appears if the strong inclination property does not hold, that is one of conditions $(H.10)$, $(H.11)$

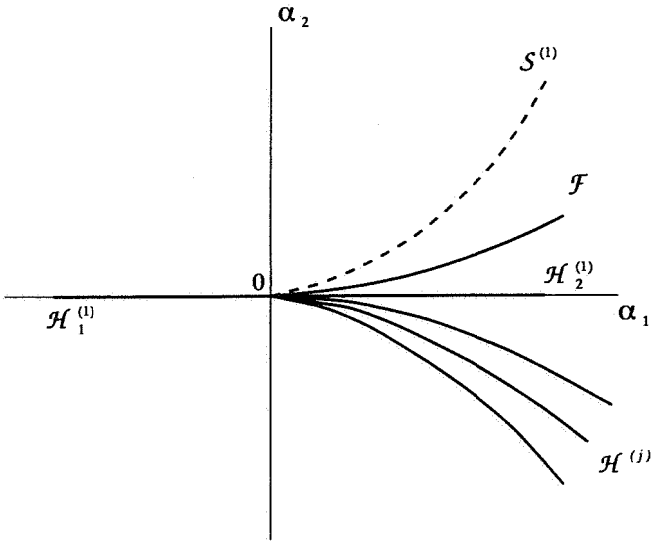

Figure 2.12: Orientation homoclinic splitting.

is violated at some parameter values, thus making the orbit *neutrally twisted* (fig. 2.13). If (H.10)

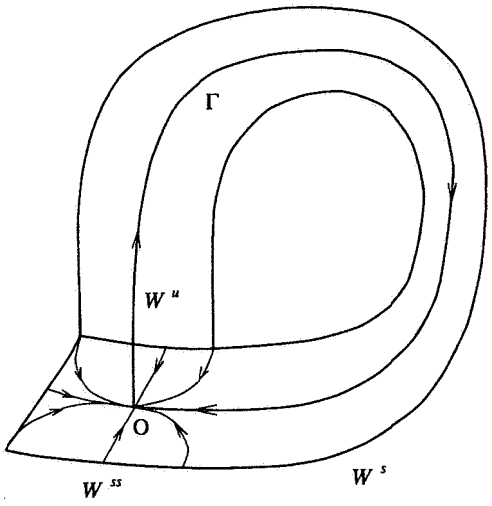

Figure 2.13: Neutrally twisted orbit at the inclination switch.

(or (H.11)) is violated, we have the so called *inclination switch with respect to the stable (unstable) manifold.* These neutrally twisted cases are clearly mapped to each other by reversing time. This bifurcation has received somewhat more attention than orbit switching and has been analysed by Yanagida (1987), Deng (1993), Kisaka, Kokubu & Oka (1993*b*), Sandstede (1993) and Homberg, Kokubu & Krupa (1993). As in the previous case, there are several sub-cases depending on the location of the eigenvalues. Suppose that the system (2.1) is three-dimensional and the eigenvalues are ordered as

$$\mu_2 < \mu_1 < 0 < \lambda_1.$$

If $\lambda_1 < |\mu_1|$, then the parametric portrait of the system contains no bifurcation curves except the primary homoclinic branch $\mathcal{H}^{(1)}$. At most one saddle cycle is present near the bifurcation.

If $|\mu_1| < \lambda_1 < \min(|\mu_2|, 2|\mu_1|)$, the parameter portrait is equivalent to that presented in fig. 2.11. Thus, we have the orientation homoclinic doubling. No extra bifurcations happen near the codim 2 point.

If $|\mu_1| < 2|\mu_1| < \min(\lambda_1, |\mu_2|)$ (or $|\mu_1| < |\mu_2| < \min(\lambda_1, 2|\mu_1|)$), the parametric portrait is similar to fig. 2.12. Therefore, the orientation homoclinic split takes place.

The above list of codim 2 bifurcations is by no means exhaustive. There other are codim 2 bifurcations involving homoclinic orbits. First of all, the equilibrium might have two distinct primary homoclinic orbits (see Gambaudo, Glendinning & Tresser (1985), Turaev & Shil'nikov (1986), Gambaudo (1987) and Glendinning (1988), Turaev (1988)). Another way to violate condition $(H.0)$ is to have a *heteroclinic cycle* at the critical parameter value. In this case, while moving along $\mathcal{H}$, another equilibrium approaches the homoclinic orbit whereby a heteroclinic cycle is created. The planar case has been studied by Reyn (1980). Some results on these cases in $\mathbb{R}^3$ can be found in Bykov (1977, 1980, 1993) and for the general case of two saddles in Chow, Deng & Terman (1990), Shashkov (1992). The homoclinic orbit might disappear by "shrinking" to a equilibrium as parameters approach a Bogdanov-Takens ($\mu_{1,2} = 0$) or Gavrilov-Guckenheimer ($\mu_1 = 0, \mu_{2,3} = \pm i\omega_0$) bifurcation point. There are also other possibilities, see Fiedler (1992) for some further discussion.

3. Numerical Continuation

Before numerical methods for degenerate homoclinic orbits can be introduced it is important to have a robust numerical method for the continuation of non-degenerate homoclinic orbits. Actually, such methods are known for *regular*, and, thus, for non-degenerate, homoclinic orbits subject to certain transversality conditions. As pointed out earlier, regular orbits lie in a codimension-one manifold $\mathcal{H}$ of parameter space. The aim of continuation is then to trace out curves in $\mathcal{H}$ as two parameters are varied. Boundary-value methods for such computations have been proposed and analyzed by Hassard (1980), Beyn (1990*b*, 1990*a*), Doedel & Friedman (1989), Friedman & Doedel (1991, 1993, 1993), among others. Continuation approaches based on shooting are discussed by Rodríguez-Luis et al. (1990) and Kuznetsov (1983, 1990). There now follows a review of boundary-value methods which prove to be the most effective and robust. In subsec. 3.1 we present an algorithm which is essentially due to Beyn. In subsec. 3.2 we compare this algorithm with other slightly different approaches and show that our approach is well suited for the current purposes. In sect. 4, we shall then consider how the algorithm behaves when one encounters the boundary of $\mathcal{H}_i$, *i.e.* at a codimension-two homoclinic points. Details of numerical implementation are confined to sect. 5.

3.1 Location and Continuation of Regular Homoclinic Orbits

To begin with, suppose that only one active parameter is chosen, so that there are isolated parameter values at which regular homoclinic orbits occur. These isolated parameter values, together with approximations to the homoclinic orbits there, may be sought numerically by continuing periodic solutions to large period or by using shooting (see, for example, Doedel & Kernévez (1986), Kuznetsov (1983, 1990), Friedman, Doedel & Monteiro). The problem of computing these isolated *starting solutions* for continuation will also be addressed in sect. 5. Instead we focus here on a boundary-value approach to computing homoclinic parameter values and the corresponding homoclinic solutions. Without loss of generality, suppose that the equilibrium in question is the origin.

We seek a solution $(x, \alpha) \in C^1(\mathbb{R}, \mathbb{R}^n) \times \mathbb{R}$ that solves

$$\dot{x}(t) = f(x(t), \alpha), \tag{3.1}$$

$$x(t) \to 0 \text{ as } t \to \pm\infty. \tag{3.2}$$

Since any time shift of a solution to (3.1), (3.2) is still a solution, a condition is required to fix the phase. Suppose that some initial guess $\tilde{x}(t)$ for the solution is known (see below), then the following integral phase condition

$$\int_{-\infty}^{\infty} \dot{\tilde{x}}^{\mathrm{T}}(t)[x(t) - \tilde{x}(t)]dt = 0 \tag{3.3}$$

is a necessary condition for a minimum of the L_2-distance between x and $\tilde{x}$ over time shifts (Doedel 1981).

Suppose that $\gamma(t)$ corresponds to a regular homoclinic orbit of (3.1) at $\alpha = 0$ and that an extra transversality with respect to the parameter takes place:

$$\int_{-\infty}^{\infty} \psi^{\mathrm{T}}(t) \frac{\partial f}{\partial \alpha}(\gamma(t), 0) dt \neq 0, \tag{3.4}$$

where $\psi(t)$ is a unique (up to a scalar multiplication) bounded solution of the *adjoint variational equation*: $\dot{z} = -B^{\mathrm{T}}(t)z$. Note that (3.4) essentially says that the parameter α is not "badly chosen" so that the α-axis lies tangent to $\mathcal{H}$ in a parameter plane. This condition explicitly specifies which systems depend "generically" on one parameter in Shil'nikov's Theorems. Assume that the initial guess $\tilde{x}(t)$ satisfies (3.3) with $x(t) = \gamma(t)$, and

$$\int_{-\infty}^{\infty} \dot{\tilde{x}}^{\mathrm{T}}(t)\dot{\gamma}(t) dt \neq 0. \tag{3.5}$$

Condition (3.5) ensures that $\tilde{x}$ is not badly chosen to lie orthogonal to solutions on $\mathcal{H}$. Then, Beyn (1990*b*, prop. 2.1,thm. 2.1) has shown that (3.1)–(3.3) is a well-posed problem and that $(\gamma, 0)$ is its regular solution in $C^1(\mathbb{R}, \mathbb{R}^n) \times \mathbb{R}$.

The boundary-value problem (3.1)–(3.3) defined on an infinite time-interval can be approximated by truncation to a finite interval $[-T, T]$, with suitable boundary conditions as follows. Suppose that the constant T and an origin of t are chosen such that $p = \gamma(-T)$ and $q = \gamma(T)$ are sufficiently close to O in the local unstable and stable manifolds respectively. Then, replace (3.2) by the following *projection boundary conditions*:

$$L_s(\alpha)x(-T) = 0, \quad L_u(\alpha)x(T) = 0. \tag{3.6}$$

where the matrices $L_s(\alpha) \in \mathbb{R}^{n,n_s}$, $L_u(\alpha) \in \mathbb{R}^{n,n_u}$ are such that the rows of $L_{s,u}(\alpha)$ form a basis for the stable and unstable eigenspaces respectively of $A^{\mathrm{T}}(\alpha)$ where $A(\alpha) = (D_x f)(0, \alpha)$. These boundary conditions place the solution at the two end points in the stable and unstable eigenspaces of $A(\alpha)$. According to the Stable and Unstable Manifold Theorem, the true homoclinic orbit will be tangent to these spaces as $T \to \infty$. Finally, take the phase condition of the truncated problem to be

$$\int_{-T}^{T} \dot{\tilde{x}}^{\mathrm{T}}(t)[x(t) - \tilde{x}(t)] dt = 0. \tag{3.7}$$

To set up some notation, let

$$\{v_1^*(\alpha), \ldots, v_{n_s}^*(\alpha)\}, \quad \text{and} \quad \{w_1^*(\alpha), \ldots, w_{n_s}^*(\alpha)\}$$

be bases of the stable and unstable eigenspaces respectively of $A^{\mathrm{T}}(\alpha)$ such that each v_i (or w_i) is in the generalized eigenspace corresponding to all eigenvalues μ (respectively λ) with $\mathrm{Re}\{\mu\} = \mathrm{Re}\{\mu_i\}$ ($\mathrm{Re}\{\lambda\} = \mathrm{Re}\{\lambda_i\}$) and, if

$$V^* = [v_1^* | \ldots | v_{n_s}^*], \quad W^* = [w_1^* | \ldots | w_{n_u}^*],$$

then

$$A^{\mathrm{T}} = [V^* | W^*]^{-1} J [V^* | W^*]$$

where J is a real canonical form of A^{T}. For example, if μ_i (or λ_i) is real and simple then v_i^* (w_i^*) is a true eigenvector of A^{T}, and if μ_i, μ_{i+1} (or λ_i, λ_{i+1}) form a simple complex conjugate pair then v_{i+1}^* and v_i^* (w_{i+1}^* and w_i^*) are the real and imaginary parts of an eigenvector corresponding to μ_{i+1} (λ_i). For use later, let

$$\{v_1, \ldots, v_{n_s}\}, \quad \text{and} \quad \{w_1, \ldots, w_{n_u}\}$$

be vectors spanning the stable and unstable eigenspaces of A which are defined analogously to the w_i^* and v_i^* with respect respect to the eigenvalues $\mu_1, \ldots, \mu_{n_s}$ and $\lambda_1, \ldots, \lambda_{n_u}$.

We suppose that $V^*(\alpha)$, and $W^*(\alpha)$ are calculated explicitly (with no continuity in α assumed) by a 'black box' routine each time the boundary conditions (3.6) need to be evaluated. In order to have a well-posed problem, however, it is necessary for the boundary conditions to be smooth with respect to α. The following technique is shown in Beyn (1990*b*, app. C) to lead to boundary conditions that are as smooth as $D_x f$. Suppose that W^* and V^* were last evaluated at at $\tilde{\alpha}$ which is such that $A(\alpha)$ is hyperbolic in a ball centered at $\tilde{\alpha}$ that contains the value α at which the boundary conditions are now required. Then there exist unique solutions to $U_s(\alpha) \in \mathbb{R}^{n_s,n_s}$ and $U_u(\alpha) \in \mathbb{R}^{n_u,n_u}$ to the linear systems

$$U_s(\alpha)[V^*(\alpha)^{\mathrm{T}}V^*(\tilde{\alpha})] = V^*(\tilde{\alpha})V^*(\tilde{\alpha})^{\mathrm{T}}, \quad U_u(\alpha)[W^*(\alpha)^{\mathrm{T}}W^*(\tilde{\alpha})] = W^*(\tilde{\alpha})W^*(\tilde{\alpha})^{\mathrm{T}}. \tag{3.8}$$

Solving (3.8) and taking

$$L_s(\alpha) = U_s(\alpha)V^*(\alpha)^{\mathrm{T}}, \quad L_u(\alpha) = U_u(\alpha)W^*(\alpha)^{\mathrm{T}} \tag{3.9}$$

achieves the desired smoothness.

It is not difficult to see that the truncated problem (3.1),(3.6)–(3.9) is formally well posed since there are $n+1$ unknowns (the vector-function $x(t)$ and the scalar α) which equals the number of boundary or integral conditions (3.6), (3.7). In fact, one has the following theorem.

Theorem 3.1 (Beyn (1990a, thm. 3.1, cor. 3.1)) *Let $\gamma(t)$ be a regular homoclinic orbit of* (3.1) *at $\alpha = 0$, such that* (3.4) *holds. Suppose $\tilde{x}(t)$ is such that* (3.3) *is satisfied with $x(t) = \gamma(t)$ and* (3.5) *holds. Finally, let $\tilde{\alpha}$ be close to 0 and $L_{s,u}$ used in* (3.6) *be computed via* (3.8) *and* (3.9).

Then, for T sufficiently large, there exist constants $\rho, C > 0$ and a phase shift $\theta_T \in [-\rho, \rho]$ such that there exists a solution $(\bar{x}, \bar{\alpha})$ to the truncated boundary value problem (3.1), (3.6)–(3.9) *that is unique in the ball*

$$\left\{(x,\alpha) \in C^1([-T,T],\mathbb{R}^n) \times \mathbb{R} : \|x - \gamma\,|_{[-T,T]}\,\|_1 + |\alpha| \le \rho\right\},$$

and satisfies the following error estimate

$$\|\bar{x} - \hat{\gamma}\|_1 + |\bar{\alpha}| \le C \exp(-\min\{|\mu|T, \lambda T\}), \tag{3.10}$$

where $Re\{\mu_1\} < \mu < 0$ and $0 < \lambda < Re\{\lambda_1\}$, $\hat{\gamma}(\tau) = \gamma(\tau + \theta_T)$, and $\|.\|_1$ denotes the usual C^1 norm.

A similar result is proved in Friedman & Doedel (1991) for a truncated problem with slightly different boundary conditions but which can be used on a wider class of heteroclinic problems. Improvements to the error estimates and extensions to non-hyperbolic equilibria have been considered by Friedman (1993) and Schecter (1993*a*, 1993*b*).

The algorithm (3.6)–(3.9) can now easily be applied within a continuation framework, by freeing an additional parameter α_2 in order to compute the curve $\mathcal{H}^{(1)}$ of homoclinic orbits. The initial guess $\tilde{x}$ used in (3.7) is taken to be the previously computed solution on the curve, while $\tilde{\alpha}$ are the previous parameter values. More precisely, let $\alpha = (\alpha_1, \alpha_2) \in \mathbb{R}^2$ and suppose that $\gamma(t)$ is a regular homoclinic orbit of (2.1) at $\alpha = 0$. Then, under appropriate transversality conditions like (3.4) and (3.5) there exists, in a neighbourhood of $(\gamma, 0)$, a unique solution branch of (3.1)–(3.3)

$$(x_s, \alpha(s)) \in C^1(\mathbb{R}, \mathbb{R}^n) \times \mathbb{R}^2,$$

for each s within some interval, such that $(x_0, \alpha(0)) = (\gamma, 0)$. Notice that this gives a direct proof of the existence of $\mathcal{H}^{(1)} = \{\alpha \in \mathbb{R}^2 | \alpha = \alpha(s)\}$.

Moreover, for sufficiently large $|T|$, there exists a unique solution branch

$$(\bar{x}_s, \bar{\alpha}(s)) \in C^1([-T,T],\mathbb{R}^n) \times \mathbb{R}^2,$$

such that $(\bar{x}_0, \bar{\alpha}(0)) = (\bar{x}, \bar{\alpha})$, of the truncated problem (3.1),(3.6)–(3.9) approximating $(x_s, \alpha(s))$ in $[-T, T]$ with a desired accuracy. An error estimate similar to (3.10) can also be given (see Beyn (1990*b*), Friedman & Doedel (1993)). We denote by $\overline{\mathcal{H}}^{(1)}$ the approximation of the exact homoclinic curve by $\{\alpha | \alpha = \bar{\alpha}(s)\}$ resulting from the truncated solution.

In sect. 5 below we present results obtained by implementing the above algorithm using AUTO (Doedel (1981), Doedel & Kernévez (1986), Doedel, Keller & Kernévez (1991*a*, 1991*b*)). The parameter s can be considered as the pseudo-arclength continuation parameter employed by AUTO.

3.2 Variations In Approach

Extension to non-trivial equilibria Suppose now that the equilibrium in question is not the origin but is some $x_O(\alpha)$ which is not known *a priori*. Then (Friedman & Doedel 1991) one can include $x_O \in \mathbb{R}^n$ as n extra scalar unknowns, with the addition of the n equations

$$f(x_O, \alpha) = 0 \tag{3.11}$$

to the system being solved. The matrices $A = (Df_x)(x_O(\alpha), \alpha), A^{\mathrm{T}}$ and vectors v_i, v_i^*, w_i, w_i^* all now depend on x_O. The algorithm (3.6)–(3.9) is virtually unchanged but one replaces $A(\alpha)$ etc. by $A(x_O(\alpha), \alpha)$ and the boundary conditions (3.6) by

$$L_s(x_O(\alpha), \alpha)(x(-T) - x_O) = 0, \quad L_u(x_O(\alpha), \alpha)(x(T) - x_O) = 0. \tag{3.12}$$

For simplicity of exposition, we henceforth resume the supposition that $x_O \equiv 0$.

Projection versus explicit boundary conditions Friedman & Doedel (1991) use, instead of the projection boundary conditions (3.7), *explicit boundary conditions*

$$x(-T) = \epsilon_0 \sum_{i=1}^{n_u} c_{0i} w_i, \quad \sum_{i=1}^{n_u} c_{0i}^2 = 1, \quad x(T) = \epsilon_1 \sum_{i=1}^{n_s} c_{1i} v_i, \quad \sum_{i=1}^{n_s} c_{1i}^2 = 1, \tag{3.13}$$

where $\epsilon_0, \epsilon_1 > 0$ and c_{0i}, c_{1i} are extra unknown scalars introduced to counterbalance replacing n boundary conditions by $2n$. The numerical problem to be solved is then (3.1), subject to (3.7) and (3.13). There are also other possibilities of an algorithm based on these boundary conditions. First, one could fix ϵ_0 and ϵ_1 but now let T vary. A count of the boundary conditions and unknowns shows that there is no longer any need for a phase condition (the phase is fixed by the choice of ϵ_0). Alternatively, fix T and ϵ_0, say, and allow ϵ_1 to vary, again with no phase condition. This latter method works well for problems where the unstable manifold is one dimensional. In this case the left-hand boundary condition can be written completely explicitly as

$$x(-T) = \epsilon_0 w_1, \tag{3.14}$$

whereas at the right-hand endpoint one can use projection, which reduces to a single equation

$$\langle w_1^*, x(T) \rangle = 0. \tag{3.15}$$

Notice that the implementation of the boundary conditions (3.14) and (3.15) requires only the eigenvectors w_1 and w_1^*.

In general, however, projection conditions are advantageous because they avoid the extra scalar unknowns c_{0i}, c_{1i}. It is also unclear whether the coefficients c_{0i} and c_{1i} would vary smoothly through a parameter value at which there are double eigenvalues of A. At such a transition two vectors w_j and w_{j+1}, say, change from being real eigenvectors to being the real and imaginary parts respectively of a complex eigenvector (if $j = 1$, this is precisely one of the codimension-two situations that we shall be interested in computing). It should be remembered that the normalisation (3.8), (3.9) overcomes this difficulty for projection boundary conditions.

Computation versus continuation of eigenvectors In Doedel and Friedman's approach, stable and unstable eigenbases of A (or A^{T} if projection conditions are used) are solved for as part of the continuation process. In the case where all the eigenvalues are real, this amounts to solving n^2 extra algebraic equations

$$A(\alpha)v_i = \mu_i v_i, \quad i = 1, \ldots n_s, \quad A(\alpha)w_i = \lambda_i w_i, \quad i = 1, \ldots n_u, \tag{3.16}$$

for the $n^2 + n$ scalar unknowns $\{\mu_i, v_i\}$, $i = 1, \ldots, n_s$, and $\{\lambda_i, w_i\}$, $i = 1, \ldots, n_s$, subject to the n constraints

$$\|v_i\| = 1, \quad i = 1, \ldots, n_0, \qquad \|w_i\| = 1, \quad i = 1, \ldots, n_u. \tag{3.17}$$

In the case of complex or double real eigenvalues, similar defining conditions can be written down for the v_i's and w_i's. In contrast, in our algorithm, we assume that the eigenvalues and eigenvectors of $A(\alpha)$ (and $A^{\mathrm{T}}(\alpha)$) are computed explicitly whenever they are required by calling a black box eigenvalue routine. Moreover we suppose that this routine always orders the eigenvalues according to the magnitude of their real parts and returns the appropriate real vectors in the case of multiple or complex eigenvalues.

There are clearly advantages and disadvantages to the two approaches which we now briefly summarize. Clearly, computing all the eigenvalues and eigenvectors of an $n \times n$ matrix at each evaluation of the boundary conditions (3.6) or (3.13), will be computationally expensive if the continuation code requires a large number of such (at different values of α) during each continuation step. However, the computational cost involved in each evaluation is small compared with the cost of solving the boundary value problem [4]. If the eigenvectors are continued rather than computed, the cost associated with computing eigenvalues and eigenvectors is avoided, but there is different source of extra computational expense. The addition of $n^2 + n$ scalar parameters increases the size of the linear systems to be solved in a boundary-value solver and may also cause convergence problems or force a code to take smaller steps along the curve $\mathcal{H}$.

The main drawback of continuing the v_i's and w_i's is that different real systems of linear equations of the form (3.16) must be solved depending on the number of complex or multiple eigenvalues in the spectrum of A. One would, for example, have to change the defining equations if trying to continue a homoclinic orbit through a parameter value at which eigenvalues coalesce on the real axis. An algorithm which was able to vary the defining equations smoothly through any such transition would likely be cumbersome. A black box routine to compute eigenvalues and eigenvectors suffers from no such drawbacks and, as outlined earlier, using the computed vectors the projection boundary conditions can easily be made to vary smoothly provided only that the equilibrium remains hyperbolic.

Phase conditions and the selection of T The error estimate (3.10) depends crucially on the truncation interval T and on the size of real parts of the leading eigenvectors. The constant C also depends on the length of time that $\gamma(t)$ spends outside the local stable and unstable manifolds. With fixed T, the size of the error may thus vary significantly at different points along the computed curve $\mathcal{H}^{(1)}$. Beyn (1990*b*) proposes a strategy for the adaptive selection of T along $\mathcal{H}^{(1)}$ which involves monitoring an estimate to the error (3.11) and adapting T in order to keep this estimate within some prescribed bounds. Such a technique is not straightforward to implement in a standard continuation code such as AUTO.

Another approach that was mentioned in subsec. 3.2.2 in connection with explicit boundary conditions is to let T be a free parameter, with ϵ_0 fixed. Such an approach can also be implemented using projection conditions by adding the single extra fixed condition

$$\|u(-T)\| = \epsilon_0. \tag{3.18}$$

Similarly, one could replace the phase condition by fixing the solution at the right-hand endpoint

$$\|u(T)\| = \epsilon_1. \tag{3.19}$$

Solving (3.1), (3.6), (3.18) and (3.19) with T now treated as an unknown can easily be shown to be a well-posed problem, and to behave well if the time interval the homoclinic orbit spends outside of the local stable and unstable manifolds varies greatly along $\mathcal{H}^{(1)}$. However, one loses the known benefits to numerical efficiency of the integral phase condition (3.3) (see Doedel, Keller & Kernévez (1991*b*)).

Instead we propose the following pragmatic approach. It is always possible to increase the accuracy of a homoclinic orbit by fixing one of the original parameters (α_2, say) and following the solution with T as the continuation parameter, Hence, if one monitors the accuracy of the homoclinic orbit along $\mathcal{H}$, and it is found that the solution becomes inaccurate, then one can stop and continue for several steps in T until a certain accuracy threshold is met. One crude way of monitoring the error would be to introduce two new *free* parameters $\epsilon_{0,1}$ and add the scalar equations (3.18), (3.19) to the system being solved. Then choose two thresholds $\delta_{1,2} > 0$ (typically $\delta_1 \ll \delta_2$ to avoid having to use this device too often). Monitor $\epsilon_{0,1}$ along $\mathcal{H}$ until

$$\max\{\epsilon_0, \epsilon_1\} > \delta_2,$$

[4] AUTO, for example, uses orthogonal collocation and the linear systems that one solves at each iteration in a continuation step are approximately of size $NTST \times NCOL \times n$ where $NTST$ is the number of mesh intervals and $NCOL$ the number of discretisation points per interval. Typically $NTST \times NCOL \sim$ 100–200.

at which point start continuation in T of exactly the same set of equations (3.1), (3.6), (3.18) and (3.19) until

$$\max\{\epsilon_0, \epsilon_1\} < \delta_1.$$

The computation of $\mathcal{H}^{(1)}$ can then be restarted from this new solution with a higher value of T. It may sometimes also be advantageous to decrease T.

We mention finally that there are other possibilities for phase conditions, for example Friedman and Doedel use

$$\int_{-T}^{T} \left(\dot{x}(t) - \dot{\tilde{x}}(t)\right)^{\mathrm{T}} \ddot{x}(t)dt = \int_{-T}^{T} \left(f(x(t),\alpha) - f(\tilde{x}(t),\tilde{\alpha})\right)^{\mathrm{T}} (Df_x)(x(t),\alpha) f(x(t),\alpha)dt = 0$$

which minimizes the L_2-distance between $\dot{\gamma}$ and $\dot{\tilde{x}}$. Such a condition works better than (3.8) for heteroclinic connections between distinct equilibria x_1 and x_2 which vary with α.

4. Numerical Treatment of Codimension-Two Homoclinic Orbits

4.1 Continuation Through Degeneracies

Our aim is to develop numerical methods to analyze the crossing of the boundary of a region $\mathcal{H}_i$ along a curve of homoclinic orbits, corresponding to one of the degeneracies described in subsec. 2.2. It is clear from sect. 3.1 that the numerical method described there will be able to continue paths of homoclinic orbits through such a boundary provided that the homoclinic orbit in question remains *regular*. In particular, the path of primary homoclinic orbits may be followed through each codim 2 point corresponding to a degeneracy in the eigenvalues of a hyperbolic equilibrium or to the more global orbit-switching or inclination-switching bifurcations. Note that the algorithm will not be "confused" by the presence of double homoclinic orbits, because such orbits, while close to the primary orbit in phase space, are not close as functions of time (and hence not close in the norm used in (3.10)). The algorithm will, however, break down if the condition $(H.1)$ is violated, *i.e.* at a saddle-node homoclinic orbit or a Hopf-Shil'nikov point. This failure is not surprising because codim 2 points are end points of curves of homoclinic orbits to hyperbolic equilibria (see subsecs. 2.2.6, 2.2.7). We now consider what would happen to the numerical solution at such points.

Consider first a saddle-node homoclinic orbit; specifically, a point on $\mathcal{H}^{(1)}$ at which the degeneracy (2.8) occurs. With reference to fig. 2.8, notice that a differentiable curve of homoclinic orbits $(\mathcal{H}^{(1)} - s_2)$ passes through the bifurcation point, albeit to a saddle on one side of the bifurcation and to a saddle-node on the other. Along such a curve, the eigenvalues of the equilibrium will vary differentiably and hence, using (3.8),(3.9), the truncated boundary conditions (3.6) can be made to vary differentiably. Note, however, that the projection boundary conditions place the left-end point on the *stable* eigenspace whereas the homoclinic orbit along s_2 is tangent to the *center* eigenspace as $t \to \pm\infty$. Moreover, as $\mu_1 \to 0$, the error estimate (3.10) becomes $O(1)$ for fixed T. Clearly then, the numerical method (3.1),(3.6)–(3.9) will not be able to compute such homoclinic orbits. Numerical methods have been devised to deal with the case of homoclinic and heteroclinic orbits to saddle-nodes (Schecter 1993*a*, Friedman 1993, Friedman & Doedel 1993), which involve boundary conditions that use higher-order approximations to the stable, unstable and center manifolds.

The situation for the Hopf-Shil'nikov bifurcation is somewhat better. Given the degeneracy (2.9) at $\alpha = 0$, it can be seen that a smooth curve $\mathcal{P}$ exists through the codim 2 point corresponding to connecting orbits between the unstable manifold of O and the stable manifold of either O or that of the periodic orbit C. In the first case, curve $\mathcal{P}$ coincides with $\mathcal{H}_1^{(1)}$. Changing notation slightly for a moment to make plain the continuity of eigenvalues, let $\mu_{1,2}(\alpha)$ represent the eigenvalues that are purely imaginary at $\alpha_2 = 0$ and $v_{1,2}$ and $v_{1,2}^*$ be vectors spanning the corresponding eigenspaces of A and A^{T} respectively. The projection conditions (3.6) calculated via (3.8),(3.9), for $\alpha > 0$, would then place the right-hand end point in the direct sum of the stable eigenspace and the leading unstable eigenspace (*i.e.* $\mathrm{span}\{v_1, v_2, \ldots, v_{n_s+2}\}$). To first approximation, for small positive α, the stable eigenspace of the periodic orbit is equal to this direct sum. Thus, in a neighbourhood of $\alpha = 0$, we expect our algorithm to compute an approximation to the curve $\mathcal{P}$. In particular, the codim 2 point would not represent an end point of continuation.

4.2 Detection and Continuation Strategy

To detect a codimension-two point along the approximation $\overline{\mathcal{H}}^{(1)}$ to a regular homoclinic curve $\mathcal{H}^{(1)}$, requires the monitoring of certain *test functions* $\psi_j(\alpha)$. Suppose a particular degenerate homoclinic solution γ occurs at $s = 0$. A test function for this degeneracy is a smooth, real-valued function defined along $\overline{\mathcal{H}}^{(1)}$ which has a regular zero at $\bar{s}$, such that $\bar{s} \to 0$ as $T \to \infty$. If a test function ψ_j, say, is found to change sign between two s-values at which the solution is calculated along the solution branch, then numerical search procedures can be used to locate to the zero of ψ to within a given accuracy. See Seydel (1988, 1991), Doedel, Keller & Kernévez (1991*a*), Khibnik, Kuznetsov, Levitin & Nikolaev (1993) for more details on the detection of degeneracies using test functions.

Once a codim 2 point corresponding to the zero of a test function ψ_j has been detected, one can continue numerically curves of codimension-two homoclinic orbits in three parameters by restarting from the detected zero of ψ_j, freeing an additional parameter and appending the extra algebraic constraint

$$\psi_j(x, \alpha) = 0 \tag{4.1}$$

to the system being solved. The implicit function theorem guarantees that the solution $(\bar{x}_s, \bar{\alpha}(s))$, $\alpha \in \mathbb{R}^3$ to the extended problem (3.1),(3.6)–(3.9), (4.1) exists locally. By monitoring other test functions along $(\bar{x}_s, \bar{\alpha}(s))$, codimension-three points that correspond to non-degeneracy conditions from $(H.1)$–$(H.11)$ failing simultaneously can be approximately detected. In principle, the strategy can be extended to compute curves of codim 3 points as four parameters are allowed to vary.

4.3 Test Functions

We consider each degeneracy described in subsecs. 2.2.1–2.2.9 in turn. In each case we suppose that the degeneracy occurs at $s = 0$ along a solution branch $(x_s, \alpha(s))$ of (3.1)–(3.3) and shall derive a test function which we show to be smooth along the solution branch $(\bar{x}_s, \bar{\alpha}(s))$ of the truncated problem (3.1),(3.6)–(3.9) and to have a regular zero near $s = 0$. Note that in the case of the inclination switch, additional equations will need to be added to (3.1),(3.6)–(3.9) (together with suitable boundary conditions) in order to be able to compute the twist type of the homoclinic orbit. Recall from subsec. 2.2.1 that the bifurcation scenario at resonant eigenvalues also depends on the twist type, and so it may also be desirable to solve these additional equations if such information is required at the bifurcation point.

Note also that each test function we shall define will depend only on the linearization at O and on functions of the solution evaluated at $t = -T$ or T. This feature of the test functions will be important for numerical implementation (see sect. 5).

Resonant eigenvalues Suppose that (2.3) holds at $s = 0$. In this case we take

$$\psi_1 = \mu_1 + \lambda_1. \tag{4.2}$$

Provided the leading eigenvalues of A remain real and simple, then it is well known that they depend smoothly on α, in which case ψ_1 given by (4.2) is a smooth function. Also, if the extra transversality assumption

$$\frac{d\mu_1}{ds} \neq -\frac{d\lambda_1}{ds}$$

is satisfied at $s = 0$, then ψ_1 will have a regular zero there. The function (4.2) is obviously smooth for the truncated problem also and has a regular zero which approaches $s = 0$ as $T \to \infty$.

Double real leading eigenvalue If (2.4) holds at $s = 0$ then, generically, a pair of simple real eigenvalues coalesce on the real axis as s varies through zero and become complex conjugate. Suppose for definiteness that the eigenvalues are real for $s < 0$ and complex for $s > 0$. Upon writing the characteristic polynomial of A as

$$\chi(z) = (a(s)z^2 + 2b(s)z + c(s))(z - \mu_2)\dots(z - \mu_{n_s})(z - \lambda_1)\dots(z - \lambda_{n_u}),$$

where μ_1 and μ_2 are the eigenvalues of the stated quadratic factor, then it is well known that the coefficients a, b, c depend smoothly on s. Moreover, so does the discriminant

$$D = b^2 - ac.$$

But, for $s < 0$, $D = \frac{1}{4}a^2(\mathrm{Re}\{\mu_1\} - \mathrm{Re}\{\mu_2\})^2$ and, for $s > 0$ $D = -\frac{1}{4}a^2(\mathrm{Im}\{\mu_1\} - \mathrm{Im}\{\mu_2\})^2$. Therefore we take as a test function

$$\psi_2 = \begin{cases} (\mathrm{Re}\{\mu_1\} - \mathrm{Re}\{\mu_2\})^2, & \mathrm{Im}\{\mu_1\} = 0, \\ -(\mathrm{Im}\{\mu_1\} - \mathrm{Im}\{\mu_2\})^2, & \mathrm{Im}\{\mu_1\} \neq 0, \end{cases} \tag{4.3}$$

which the above arguments show to be smooth with respect to s and to have a regular zero at $s = 0$ provided

$$\frac{dD(s)}{ds} \neq 0.$$

In the time-reversed situation we take a test function

$$\psi_3 = \begin{cases} (\mathrm{Re}\{\lambda_1\} - \mathrm{Re}\{\lambda_2\})^2, & \mathrm{Im}\{\lambda_1\} = 0, \\ -(\mathrm{Im}\{\lambda_1\} - \mathrm{Im}\{\lambda_2\})^2, & \mathrm{Im}\{\lambda_1\} \neq 0. \end{cases} \tag{4.4}$$

The functions (4.3) and (4.4) are also smooth for the truncated problem and each has a regular zero that approaches $s = 0$ as $T \to \infty$.

Saddle-focus cases For each degeneracy (2.5)–(2.6) that involves only simple eigenvalues, one can easily define smooth test functions, since simple eigenvalues depend smoothly on the parameters. The condition for these functions to have have regular zeros at the appropriate degeneracy will be a transversality condition on the eigenvalues that in each case can be expressed as the derivative of the test function with respect to s being non-zero. These conditions hold generically. Specifically we take for both exact and truncated problems:

neutral saddle-focus

$$\psi_4 = \mathrm{Re}\{\mu_1\} + \mathrm{Re}\{\lambda_1\};$$

neutrally-divergent saddle-focus

$$\psi_5 = \mathrm{Re}\{\mu_1\} + \mathrm{Re}\{\mu_2\} + \mathrm{Re}\{\lambda_1\}, \quad \text{or}$$
$$\psi_6 = \mathrm{Re}\{\lambda_1\} + \mathrm{Re}\{\lambda_2\} + \mathrm{Re}\{\mu_1\};$$

three leading eigenvalues

$$\psi_7 = \mathrm{Re}\{\mu_1\} - \mathrm{Re}\{\mu_3\}, \quad \text{or}$$
$$\psi_8 = \mathrm{Re}\{\lambda_1\} - \mathrm{Re}\{\lambda_3\}.$$

Non-hyperbolic equilibria Here we define test functions for detecting saddle-node or Hopf-Shil'nikov homoclinic orbits under the *presupposition* that a continuous path of solutions to some truncated numerical problem can be followed through the codim 2 singularity. Recall from the discussion in sect. 4.1, that, at least in the saddle-node case, such a path cannot be continued using (3.6)–(3.10). In the previous notation it was assumed that $\mathrm{Re}\{\lambda_1\} > 0$, so that a non-hyperbolic equilibrium always satisfies $\mathrm{Re}\{\mu_1\} = 0$. In an application, however, it is equally likely that on the real part of an *unstable* eigenvalue approaches zero on the path of homoclinic orbits leading to the non-hyperbolic equilibrium. Hence we consider two separate test functions

$$\psi_9 = \mathrm{Re}\{\mu_1\},$$
$$\psi_{10} = \mathrm{Re}\{\lambda_1\}$$

each of which will detect either Hopf or saddle-node bifurcations along a homoclinic curve. Note that the transversality conditions for a zero of $\psi_{9,10}$ are the same as the transversality conditions for the corresponding local bifurcations (Guckenheimer & Holmes 1983). A remark similar to those given before on the exact and truncated problems can be made.

We now move on to the cases which cannot be detected merely by monitoring functions of eigenvalues. Henceforth in this section we suppose that the leading eigenvalues of A are both real and simple.

Orbit switch Recall from sect. 2 the definitions of the points p,q and unit vectors $e^{\pm}$. Suppose that $(H.9)$ is violated for $s = 0$ and that, as depicted in fig. 2.10, the unit vector e^+ switches components of the leading stable eigenvector v_1, as s passes through zero. Then, clearly, the function

$$\langle e^+(s), v_1(\alpha(s))\rangle$$

changes sign for the exact problem (3.1)–(3.3), provided that v_1 is chosen to depend continuously on s. This function is, however, discontinuous at $s = 0$ and, thus, can not be used as a test function. Consider instead the homoclinic solution $\gamma(t)$ to (3.6) at the point $q = \gamma(T)$. As s varies, due to classical continuous dependence of solutions on parameters and initial conditions for ordinary differential equations over a *finite* time interval, q will vary smoothly with s. Moreover, $\dot\gamma(T)$ varies smoothly with s and remains bounded at $s = 0$. Hence, so does

$$\langle e(T), v_1(\alpha(s))\rangle = \left\langle \frac{f(x(T),\alpha)}{\|f(x(T),\alpha)\|}, v_1(\alpha)\right\rangle\Bigg|_{x=\gamma_s,\alpha=\alpha(s)}.$$

Moreover, for T sufficiently large, the above function has a zero for s near zero and, due to the error estimate (3.10), so does the same function evaluated on the solution branch $(\bar x_s, \bar\alpha(s))$ to the numerical problem (3.1),(3.6)–(3.9).

These arguments show that the function

$$\psi_{12} = \left\langle \frac{f(x(T),\alpha)}{\|f(x(T),\alpha)\|}, v_1(\alpha)\right\rangle$$

is a test function for orbit switching with respect to the stable manifold and

$$\psi_{11} = \left\langle \frac{f(x(-T),\alpha)}{\|f(x(-T),\alpha)\|}, w_1(\alpha)\right\rangle$$

is a test function for orbit switching it with respect to the unstable manifold.

Inclination switch Methods for the numerical detection of inclination switching have first been proposed by Kuznetsov (1990) for saddles with one-dimensional unstable manifolds (see (Kuznetsov 1991) for a more detailed treatment and a numerical example). Here we present a test function that is valid in the general case. Recall, from sect. 2, the definitions of the tangent spaces $Z(t) = X(t)+Y(t)$, the unit vector $e(t)$, and the Jacobian $B(t)$ of f around the homoclinic orbit. All these objects depend on s, which dependence will not indicated below for simplicity. If properties $(H.8)$, $(H.9)$ are satisfied, then the space $X(t)$ is spanned by $n_s - 1$ tangent vectors

$$\{v_2(t),\ldots,v_{n_s}(t)\}, \quad \text{where} \quad \lim_{t\to\infty} v_i(t) = v_i,$$

and the unit vector $e(t)$, while $Y(t)$ is spanned by $n_u - 1$ tangent vectors

$$\{w_2(t),\ldots,w_{n_u}(t)\}, \quad \text{where} \quad \lim_{t\to\infty} w_i(t) = w_i,$$

and $e(t)$. These vectors can be selected to depend continuously on t.

The normal vector $z(t)$ to $Z(t)$ is the unique bounded solution (to within a scalar multiple) of the *adjoint variational equation* around the homoclinic orbit

$$\dot z = -B^{\mathrm T}(t)z,$$

where, recall, $B(t) = (D_x f)(\gamma(t),\alpha(s))$. Note that $\lim_{|t|\to\infty} B^{\mathrm T}(t) = A^{\mathrm T}$. To avoid strong divergence of solutions of the adjoint variational equation, consider, following the approach by Kuznetsov (1991), the nonlinear, *normalized* adjoint variational equation

$$\dot u = -B^{\mathrm T}(t)u + \langle B^{\mathrm T}(t)u, u\rangle u. \tag{4.5}$$

The unit normal to $Z(t)$,

$$u(t) = \frac{z(t)}{\|z(t)\|}$$

satisfies (4.5) and has the properties

$$\langle u(t), e(t)\rangle = 0, \qquad \forall t \in (-\infty, \infty), \tag{4.6}$$
$$\langle u^+, w_i\rangle = 0, \qquad i = 2, \ldots, n_u, \tag{4.7}$$
$$\langle u^-, v_i\rangle = 0, \qquad i = 2, \ldots, n_s, \tag{4.8}$$

(Sandstede 1993), where

$$u^{\pm} = \lim_{t \to \mp\infty} u(t).$$

Suppose that eigenvectors v_1^* and w_1^* of A^{T} are of unit length and are chosen so that

$$\langle v_1^*, e^-\rangle \geq 0, \quad \langle w_1^*, e^+\rangle \geq 0.$$

Then, if $(H.10), (H.11)$ are satisfied, we have

$$u^+ = \pm v_1^* \quad \text{and} \quad u^- = \pm w_1^*,$$

and the homoclinic orbit is twisted or non-twisted according to the sign of the product

$$\Delta = \langle u^+, v_1^*\rangle\langle u^-, w_1^*\rangle. \tag{4.9}$$

Now suppose that $(H.10)$ (or $(H.11)$) is violated at $s = 0$ and the transversality condition is satisfied that e^+ (respectively e^-) switches to the opposite component of v_1^* (w_1^*) as s passes through zero. Then the product (4.9) will change sign. Following Kisaka et al. (1993*b*), we say that an inclination switch takes place *with respect to the stable manifold* if the first scalar product in (4.9) passes through zero and with respect to the unstable manifold if the second scalar product does so. To define a test functions for these two cases of inclination switching we use the same idea as for the orbit switch, namely the evaluation of a scalar product at the points p and q. We can then use the same arguments as before to show that this test function is smooth and will have a regular zero close to an inclination switching bifurcation of the exact problem, given the transversality condition mentioned at the start of the paragraph. Also, we compute an approximate solution to (4.5)–(4.8) by solving the equation (4.5) on the finite interval $[-T, T]$ subject to the n boundary conditions

$$\|u(-T)\| = 1, \qquad \langle u(-T), e(-T)\rangle = 0, \tag{4.10}$$
$$L_{uu}^* u(-T) = 0, \qquad L_{ss}^* u(T) = 0, \tag{4.11}$$

Here, the matrices $L_{uu}^*(\alpha) \in \mathbb{R}^{n, n_u - 1}$, $L_{ss}^*(\alpha) \in \mathbb{R}^{n, n_s - 1}$ are such that the rows of $L_{uu,ss}^*$ form a basis for the *strong* unstable and stable eigenspaces respectively of A (i.e. $\mathrm{span}\{w_2, \ldots, w_{n_u}\}$ and $\mathrm{span}\{v_2, \ldots, v_{n_s}\}$ respectively). We suppose that the boundary conditions (4.11) are computed using the technique (eqs. (3.8), (3.9)) that ensured smoothness of $L_{s,u}$ with respect to α. Hence, (4.5),(4.10),(4.11) can be shown to be a well posed problem for sufficiently large T, the solution to which tends to the true unit normal to $Z(t)$ as $T \to \infty$. Specifically then, we take

$$\psi_{13} = \langle u(-T), v_1^*\rangle$$

to detect a switch with respect to the unstable manifold, where $u(t)$ solves (4.5),(4.10),(4.11), and

$$\psi_{14} = \langle u(T), w_1^*\rangle$$

for a switch with respect to the stable manifold.

5. Numerical Results

The results in this section serve to illustrate the numerical approach presented in the previous two sections. First we elucidate how the algorithm is implemented using AUTO and also discuss how to obtain starting solutions. Then we present results on four different example systems for which the existence of certain codim 2 homoclinic orbits are already known. The results we present are not new, in general, although there are a few novel features. Also, we compute only homoclinic orbits and not the dynamics in their neighbourhood (which are often of more interest in applications), but instead give references to where a more complete picture can be found. Our aim, then, is to use these examples as "test problems" for our unified approach for locating and following codim 2 homoclinic orbits. We have chosen examples which illustrate separately the different codimension-two situations discussed in subsec. 2.2. We do not, however, consider saddle-node homoclinic orbits for the reasons outlined in subsec. 4.1, and we know of no examples in the literature of orbit-switching or three-leading-eigenvalue homoclinic bifurcations. (Deng (1993) refers to a system studied by Terman (1992) as providing an example of orbit-switching. However, we discount this example because the codim 2 homoclinic orbit exists in a singular limit and is actually a homoclinic orbit to a saddle-node.)

5.1 Details of Numerical Implementation

In this section, we show how our approach can be implemented in the software package AUTO written by E. Doedel. To use AUTO one must write a *driver* program that contains certain user-supplied subroutines which specify the particular bifurcation problem to be solved. See the manual (Doedel & Kernévez 1986) and the tutorial papers Doedel, Keller & Kernévez (1991*a*, 1991*b*) for details of the numerical methods used by AUTO, of the practicalities of using the software and for a list of its capabilities.

Continuation Among other things, AUTO can compute paths of solutions to boundary value problems with integral constraints and non-separated boundary conditions;

$$\dot{U}(\tau) = F(U(\tau),\beta), \qquad U(\cdot), F(\cdot,\cdot) \in \mathbb{R}^N,\ \beta \in \mathbb{R}^{n_{\rm free}},\ \tau \in [0,1] \tag{5.1}$$

$$b(U(0),U(1),\beta) = 0, \qquad b(\cdot,\cdot) \in \mathbb{R}^{n_{\rm bc}}, \tag{5.2}$$

$$\int_0^1 q(U(\tau),\beta)d\tau = 0, \qquad q(\cdot,\cdot) \in \mathbb{R}^{n_{\rm nin}}, \tag{5.3}$$

as $n_{\rm free}$ *free* parameters β are allowed to vary, where

$$n_{\rm free} = n_{\rm bc} + n_{\rm nin} - N + 1. \tag{5.4}$$

The function q is also allowed to depend on F, the derivative of U with respect to pseudo-arclength and on $\hat{U}$, the value of U at the previously computed point on the solution branch. Moreover, AUTO can accurately locate zeros along the solution branch of functions

$$g_j(U(0),U(1),\beta), \quad j = 1,\dots n_{\rm uszr} \tag{5.5}$$

Actually, the user-defined functions in AUTO are functions of parameters only (not necessarily just the free parameters), but only a simple modification of the user-supplied subroutine USZR in the driver program is required to enable these functions to depend also on the boundary values of U.

Suppose that we wish to continue solutions to the equations (3.1),(3.6)–(3.9) for a homoclinic orbit together with equations (4.5),(4.10),(4.11) for the normal vector to $Z(t)$, subject to $n_{\rm fix}$ constraints

$$\psi_i = 0, \quad i = i_{\rm fix\,1},\dots,i_{\rm fix\,n_{fix}},$$

where $i_{{\rm fix}\,j}$ is the label of the the jth test function that has been frozen, as $n_{\rm fix} = n_{\rm free} + 2$ parameters

$$\alpha_i, \quad i = i_{\rm free\,1},\dots i_{\rm free\,n_{free}}$$

are allowed to vary. Suppose too that we want to monitor $n_{\rm test}$ test functions

$$\psi_i, \quad i = i_{\rm test\,1},\dots,i_{\rm test\,n_{test}}.$$

Then this problem can be written in the form (5.1)-(5.5) after a suitable time shift and rescaling that identifies $t = -T$ with $\tau = 0$ and $t = T$ with $\tau = 1$. Specifically we have

$$N = 2n, \quad n_{\rm bc} = 2n + n_{\rm fix}, \quad n_q = 1, \quad U(\tau) = (x(\tau), u(\tau))^{\rm T}, \quad \beta = (\alpha_i,\ i = i_{\rm free\,1}, \ldots i_{\rm free\,} n_{\rm free}),$$

$$F(U,\beta) = \begin{pmatrix} Tf(x,\alpha) \\ -T\left([(D_x f)(x,\alpha)]^{\rm T} u - \langle [(D_x f)(x,\alpha)]^{\rm T} u, u\rangle u\right) \end{pmatrix}, \tag{5.6}$$

$$b(U(0),U(1),\beta) \quad = \quad \begin{pmatrix} L_s(\alpha)x(0) \\ L_u(\alpha)x(1) \\ \|u(0)\| - 1 \\ \langle u(0), f(x(0),\alpha)\rangle \\ L^*_{uu}u(0) \\ L^*_{ss}u(1) \\ \psi_k, k = i_{\rm fix\,1}, \ldots, i_{\rm fix\,} n_{\rm fix} \end{pmatrix},$$

$$q(U,\beta) = \dot{\hat{x}}^{\rm T}(x - \hat{x}), \quad g_i(U(0),U(1),\beta) = \psi_i,\ i = i_{\rm test\,1}, \ldots, i_{\rm test\,} n_{\rm test}.$$

Remarks

1. Note that the boundary conditions and some of the test functions depend on the vectors v_i^*, w_i^* (or v_i, w_i). These we compute explicitly each time they are required at new parameter values by calling the NAG routine F02AGF to compute all the eigenvalues and eigenvectors of $A^{\rm T}$ (or A) and then ordering the vectors according to the size of the real part of the eigenvalues. We then take the real and imaginary parts of complex eigenvectors and compute generalised eigenvectors in the case of double real eigenvalues. The normalisation technique (3.8), (3.9) is used when computing $L_{s,u}$ or $L_{ss,uu}$.

2. One of the free parameters in AUTO, $\alpha_{i_{\rm free\,1}}$ in our notation, is taken to be the *continuation parameter*, in which parameter the user can specify the (maximum, minimum and sign of) steps to be taken. Note that it is possible for one of the free parameters to be T and even to use this as the continuation parameter (cf. subsec. 3.2.4).

3. If the normal vector to $Z(t)$ is not required (*i.e.* we do not wish to compute the orientation), then the size of the system to be solved reduces to $N = n$.

4. Additional constraints, such as (3.11) or (3.18), (3.19), can be added to the boundary conditions provided additional parameters are freed. In the case of the condition (3.11) to determine the equilibrium, the extra parameters will be the n scalar unknowns x_O.

5. If a zero of a test function ψ_j, say, is detected and the locus of multiple-codimension points corresponding to zeros of
$$\psi_i, \quad i = i_{\rm test\,1}, \ldots, i_{\rm test\,} n_{\rm test}, j$$
is required as $n_{\rm free} + 1$ parameters are varied, then continuation can be restarted from this point with an extra free parameter α_j, say, and the test function ψ_j added to the boundary conditions (5.2).

6. Also, given a zero of ψ_j, it may be desirable to restart continuation at this point with different test functions $\psi_{i_{{\rm fix}\,k}}$ included in the list (5.5) of user-defined functions. For example, when computing a curve of saddle homoclinic orbits, a zero of the test function ψ_2 (or ψ_3) may be detected, *i.e.* there are double real eigenvalues. The homoclinic orbit on the other side of such a codim 2 point would then be a saddle-focus and one would want to "switch on" the saddle-focus test functions $\psi_{4,5,7}$ (respectively $\psi_{4,6,8}$) and "switch off" the test functions ψ_{11-14} which only apply in the saddle case.

7. It is also possible to add other "user defined" functions $g_j(U(0), U(1), \alpha, T)$, $j > n_{\text{test}}$, to detect points at zeroes of which the solution is required and from which continuation may be restarted. For example, the conditions which measure the distance of the solution from the equilibrium,

$$g_j = \max\{\epsilon_0, \epsilon_1\} - \delta_1, \quad g_{j+1} = \max\{\epsilon_0, \epsilon_1\} - \delta_2,$$

where $\epsilon_{0,1}$ are given by (3.18), (3.19), will be useful for the pragmatic approach discussed in subsec. 3.2.4 for the selection of T.

An AUTO driver AUTHOMCONT.F, which is available from the first author on request, has been written to implement the above algorithm for a general system in arbitrary dimensions (within the limits of storage within AUTO). The driver has been written so that only minor changes need be made to adapt it to run on new problems.

Starting solutions Two possible ways of starting the continuation of a curve of homoclinic orbits are allowed for in AUTHOMCONT.F. Firstly, data from some previously computed homoclinic orbit (and normal vector $u(t)$, if that is required) may be read into AUTO and treated as an analytically known solution. This previously computed orbit may have been obtained using shooting or, if the normal vector is not required, by following periodic orbits to large period. We refer the reader to Doedel et al. (1991*b*) and to Kuznetsov (1990, 1991) for more details on these two methods. We have not implemented more sophisticated ways of homotopying between periodic and projection boundary conditions, but see Friedman & Doedel (1993).

The second way of computing a starting solution is to use AUTO to perform a kind of shooting, as proposed by Friedman, Doedel & Monteiro (1993), in what we call an *artificial parameter* approach. We report here how this approach can be used to also obtain the normal vector for saddle homoclinic orbits. Suppose the parameter values for a homoclinic orbit are known exactly (see Friedman et al. (1993) for a specific example, using this approach, in which homoclinic parameter values are obtained as well). The basic idea is then to start with a small value of T, an approximate solution close to the origin in the leading unstable manifold and an approximate normal vector to $W^u + W^{ss}$; then to continue this solution to (3.1), (4.5) as T is increased; and, finally, to vary the initial conditions until appropriate right-hand boundary conditions are satisfied.

More specifically, introduce extra parameters

$$\epsilon_0, \quad \xi_i, \omega_i,\ i = 1, \ldots n_u, \quad \text{and} \quad \eta_i, \zeta_i,\ i = 2, \ldots, n_s,$$

and solve (5.1), where F is given by (5.6), subject to the boundary conditions

$$x(0) = \epsilon_0 \sum_1^{n_u} \xi_i w_i, \quad \sum_1^{n_u} \xi_i^2 = 1, \quad \|u(0)\| = 1, \tag{5.7}$$

$$\langle u(0), f(x(0), \alpha)\rangle = 0, \quad \langle u(0), w_i\rangle = 0,\ i = 2, \ldots n_u, \quad \langle u(0), v_i\rangle = \eta_i,\ i = 2, \ldots n_s, \tag{5.8}$$

$$\langle x(1), w_i^*\rangle = \omega_i, \quad i = 1, \ldots n_u, \quad \langle u(1), v_i\rangle = \zeta_i, \quad i = 2, \ldots n_s. \tag{5.9}$$

The boundary conditions (5.7), (5.8) specify the left-hand end point of the solution exactly, and the conditions (5.9) are projection conditions evaluated at the right-hand end point. Note that there is no integral condition. The solution we require satisfies the right-hand boundary conditions with $\omega_i = 0$, $i = 1, \ldots, n_u$ and $\zeta_i = 0$, $i = 2, \ldots, n_s$. Therefore, user-defined functions

$$g_i = \omega_i,\ i = 1, \ldots n_u, \quad g_{n_u - 1 + i} = \zeta_i,\ i = 2, \ldots n_s,$$

are included and a solution to (5.1), (5.6)–(5.9) is sought that satisfies $g_i = 0$, $i = 1, \ldots n_s + n_u - 1$. Note that there are $2n + n_s + n_u$ boundary conditions (5.7) (including the constraint on the ξ_i's), (5.8) and (5.9), and $N = 2n$ equations. Therefore, according to (5.4) we require $n_s + n_u + 1$ free parameters.

To begin with, fix ϵ_0 to be a small positive number, fix the parameters

$$\xi_i = 0,\ i = 2, \ldots, n_s, \quad \eta_j = 0,\ j = 2, \ldots, n_s,$$

and take the explicit starting solution

$$\hat{x}(\tau) = \epsilon_0 w_1 \exp(\lambda_1 \tau / T), \quad \hat{u}(\tau) = v_1^*$$

where it is assumed that $\|w_1\| = 1, \|v_1\| = 1$. Let T be the continuation parameter, and let

$$\xi_1, \quad \omega_i, \quad i = 1, \ldots, n_u, \quad \text{and} \quad \zeta_i, \quad i = 2, \ldots, n_s,$$

be the other $n_s + n_u - 1$ free parameters [5] with starting values

$$\xi_1 = 1, \quad \omega_1 = \langle \hat{x}(1), w_1^* \rangle, \quad \omega_i = 0,\ i = 2, \ldots n_u, \quad \zeta_i = 0,\ i = 2, \ldots n_s.$$

The continuation is then stopped after a suitably large value of T has been reached (which value is determined heuristically for each specific example). The parameter T is now fixed and the parameter ξ_2, say, is freed. We then continue in ξ_2 (or any of the ω_i's) until a zero of one of the ω_i's is detected (to within a desired accuracy). Once such a zero is detected, the corresponding ω_i is frozen and an additional parameter ξ_3 is freed. This process is continued until all but one of the ω_i's are zero. A final continuation in T will ensure that an approximation to the homoclinic orbit is found (since we assume that α is a homoclinic parameter value). A similar process can then be used to compute the normal vector $u(t)$, by repeatedly freeing parameters η_i and detecting zeroes of the ζ_i's until all the ζ_i's are zero. Notice that in this entire process, ϵ_0 and all the true parameters α remain fixed.

While there are no theorems to guarantee that such a method will work, we have found it to be successful in all the examples we have tried (all of which albeit have a one-dimensional unstable manifold).

5.2 The FitzHugh-Nagumo Equations: Double Real Leading Eigenvalue

The following system of PDEs is the FitzHugh-Nagumo (FHN) caricature of the Hodgkin-Huxley equations modelling the nerve impulse propagation along an axon (FitziHugh 1961, Nagumo, Arimoto & Yoshizawa 1962):

$$\begin{aligned} \frac{\partial u}{\partial t} &= \frac{\partial^2 u}{\partial x^2} - f_a(u) - v \\ \frac{\partial v}{\partial t} &= bu, \end{aligned}$$

where $u = u(x,t)$ represents the membrane potential, $v = v(x,t)$ is a phenomenological "recovery" variable, $-\infty < x < +\infty, t \geq 0$, $0 < a < 1$ and $b > 0$ are the parameters and

$$f_a(u) = u(u-a)(u-1).$$

Solitary nerve "impulses" correspond to homoclinic solutions of the ODEs

$$\left\{ \begin{aligned} \dot{U} &= W \\ \dot{W} &= cW + f_a(U) + V \\ \dot{V} &= \frac{b}{c} U, \end{aligned} \right. \tag{5.10}$$

which describe travelling-wave solutions of the FHN system of the form

$$u(x,t) = U(\xi),\ v(x,t) = V(\xi),\ \xi = x + ct,$$

[5] A slight modification is used if the unstable manifold is one-dimensional. Then the explicit condition (5.7) for $x(0)$ can be written as a single boundary condition with no artificial parameters. There is thus one less boundary condition and one less free parameter ξ_1.

where c is an *a priori* unknown wave propagation speed. Here a dot denotes differentiation with respect to "time" ξ.

The system (5.10) depends on three parameters (a, b, c) and for all $c > 0$ it has a unique equilibrium at the origin with one positive eigenvalue λ_1 and two eigenvalues $\mu_{1,2}$ with negative real parts. It is well-known that there exist parameter values for which the branch of the unstable manifold that leaves the origin into the positive octant forms a homoclinic orbit (Hastings (1976, 1982), Jones (1984)).

The equilibrium can either be a saddle or a saddle-focus with a one-dimensional unstable manifold. Double real negative eigenvalues ($\psi_2 = 0$) occur, for fixed $b > 0$, on the curve

$$D_b = \{(a, c) : c^4(4b - a^2) + 2ac^2(9b - 2a^2) + 27b^2 = 0\}. \tag{5.11}$$

A codim 2 homoclinic bifurcation has been found in (5.10) by Kuznetsov & Panfilov (1981). They calculated loci $\mathcal{H}^{(1)}$ of homoclinic orbits in the (a, c)-plane for several different fixed values of b. For sufficiently small b it was found that the homoclinic locus passes through the curve given by (5.11) twice and, because the unstable eigenspace is always determining for $c > 0$, the codim 2 bifurcation depicted in fig. 2.5 occurs both times. Fig. 5.1 presents several curves $\mathcal{H}^{(1)}$ recalculated via the methods of the present paper. To obtain starting solutions we used the artificial parameter approach. According to the description given in sec. 3.2.2, each of these codim 2 points, is the origin of an infinite number of *double* homoclinic curves. The double homoclinic orbits correspond to the so called *double-pulse waves* in the FHN system. For larger b ($b > b_{\min}$) the homoclinic locus is completely contained in the saddle-focus region. Our continuation technique allows us to find numerically this critical value $b_{\min}$ at which the two codim 2 points A_j coincide so that the curve $\mathcal{H}^{(1)}$ is *tangent* to the double-eigenvalue curve D_b (a non-transversal Belyakov bifurcation). The points $A_{1,2}$ belong to the single curve in the (a, b, c)-parameter space depicted in fig. 5.2 and the minimal value of the b-coordinate along this curve gives $b_{\min} = 0.00544656$.

The infinite number of periodic orbits and double homoclinic orbits of (5.10), corresponding respectively to periodic and double-pulse wave-train solutions of the FHN system, have been predicted independently of codim 2 arguments for FHN-type equations by Evans et al. (1982).

5.3 Chua's Electronic Circuit: Neutral Saddle-Focus and a Codim 3 Bifurcation

Khibnik, Roose & Chua (1993) consider the following system of three ODEs

$$\begin{cases} \dot{x} &= \alpha(y - \phi(x)) \\ \dot{y} &= x - y + z \\ \dot{z} &= -\beta y \end{cases}, \tag{5.12}$$

where $\phi(x) = c_1x_3 + c_2x^2 + c_3x + c_4$, which models Chua's autonomous electronic circuit (Matsumoto, Chua & Kumuro 1985) where the nonlinearity is assumed to be smooth. The parameter values

$$c_1 = \frac{1}{6}, \quad c_2 = 0, \quad c_3 = -\frac{1}{6}, \quad c_4 = 0, \tag{5.13}$$

were taken, so that (5.12) has odd symmetry (*i.e.* is invariant under the transformation $(x, y, z) \to (-x, -y, -z)$). We refer the reader to Khibnik, Roose & Chua (1993) for a description of the dynamics of this model. The only facts of relevance here are that the origin is always an equilibrium of (5.12) and that a path of homoclinic orbits to the origin emerges into the positive quadrant of the (α, β)-plane [6]; the locus terminates at a Bogdanov-Takens point when $(\alpha, \beta) = (0, 0)$. Note also that, for all $\alpha, \beta > 0$, the origin is hyperbolic and has a one-dimensional unstable manifold.

Using shooting we were able to locate an approximation to a homoclinic orbit at $(\alpha, \beta) = (0.9, 0.8246)$, over a time interval $T = 44.0$. At these parameter values the determining eigenvalue is the leading unstable one. This solution was then used as starting data for continuation using AUTO with α and β as the free parameters (and α increasing). The results are depicted in fig. 5.3. In all, four codimension-two points corresponding to zeros of a test functions ψ_i were detected. In order of increasing alpha these are:

[6] Actually, there are always a pair of symmetry-related homoclinic orbits at the relevant parameter values. It suffices to compute only one of them.

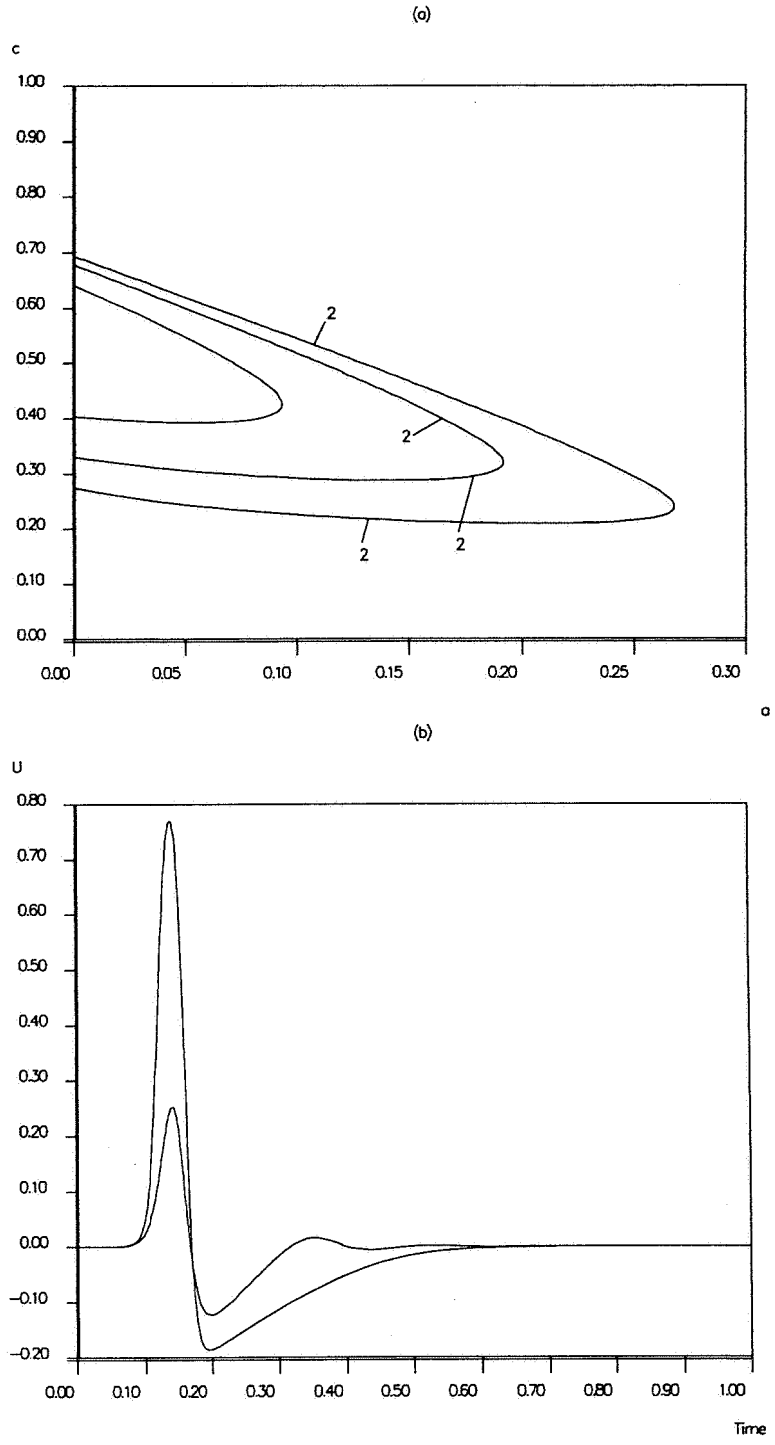

Figure 5.1: (a) Loci in the (a, c) plane of homoclinic orbits in the FitzHugh-Nagumo wave system for (from left to right) $b = 0.01, 0.005, 0.0025$. Points labelled 2 correspond to double real leading eigenvalue homoclinic orbits ($\psi_2 = 0$). (b) Travelling impulses in the saddle and saddle-focus regions for $b = 0.005$, where the time-interval ($T = 200$) has been normalised to unity.

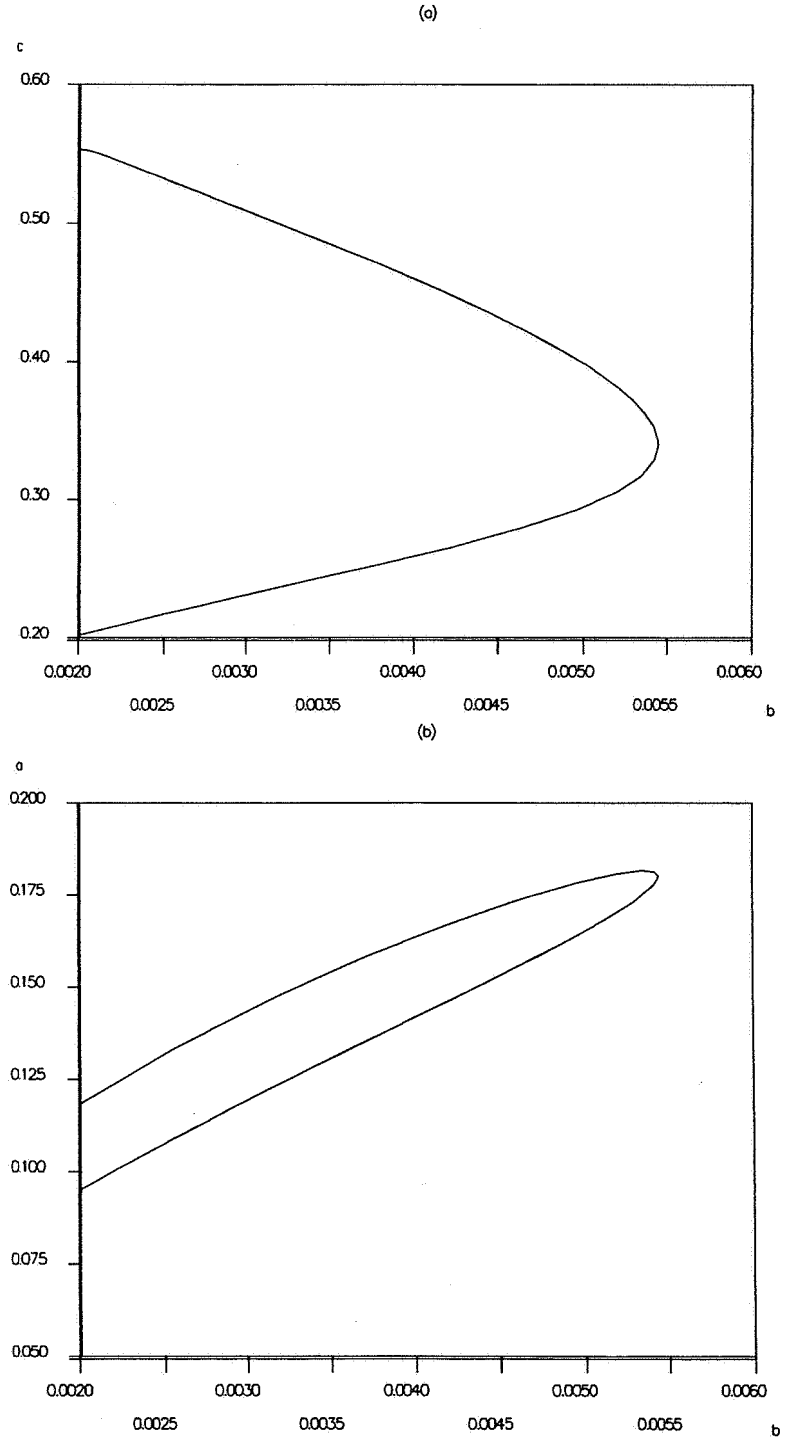

Figure 5.2: (a) Loci of double-real-leading-eigenvalue homoclinic orbits in the (b, c) and (b, a) planes.

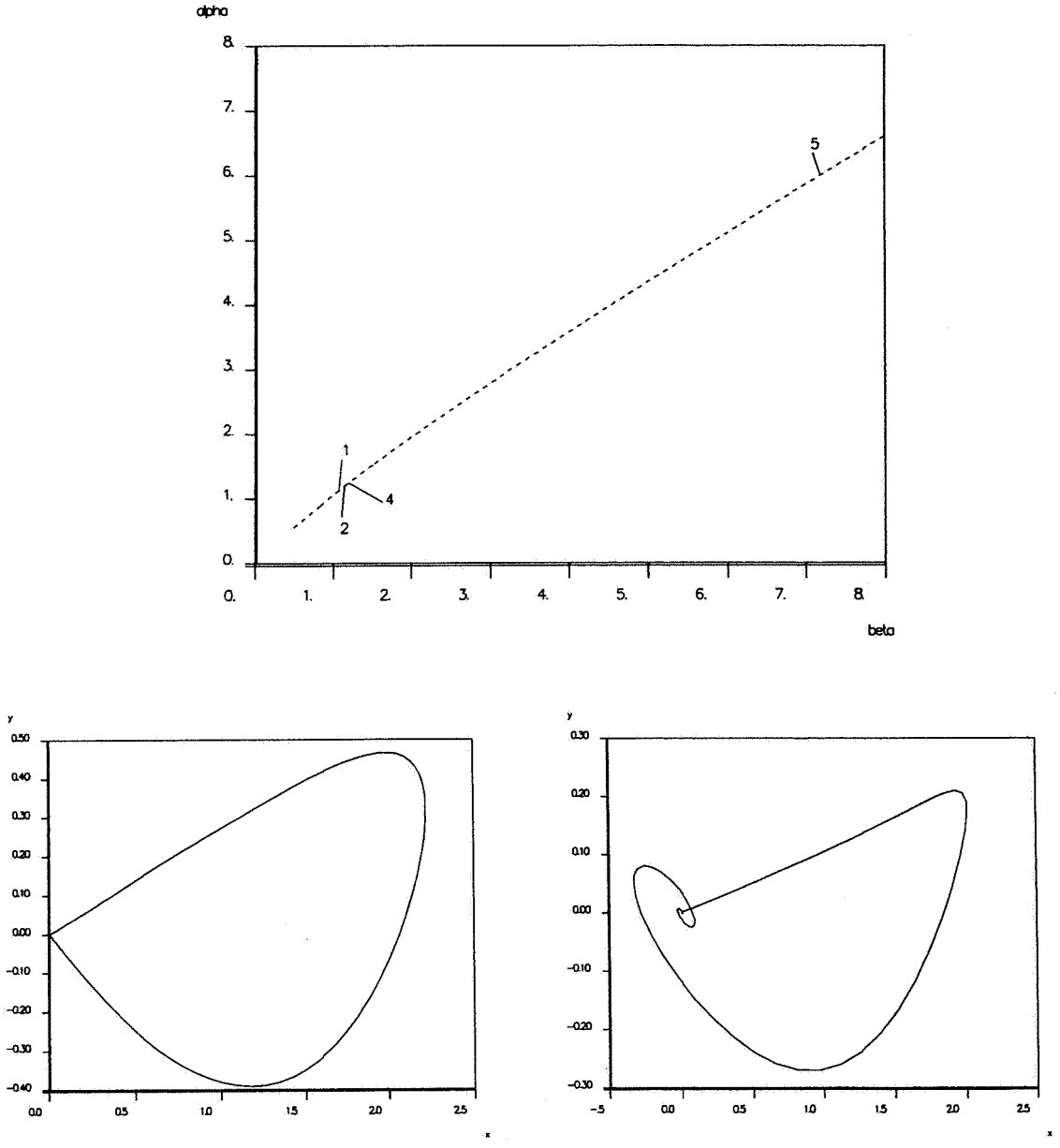

Figure 5.3: (a) Locus of homoclinic orbits in Chua's circuit; labels are the indices of the test functions which are zeroed. (b),(c) Homoclinic orbits at 1 and 5 respectively.

1. at $(\alpha, \beta) = (1.13515, 1.07379)$, neutral saddle ($\psi_1 = 0$);
2. at $(\alpha, \beta) = (1.20245, 1.14678)$, double real leading eigenvalue (with respect to stable eigenspace, which is non-determining; *i.e.* $\psi_2 = 0$);
3. at $(\alpha, \beta) = (1.74917, 1.76178)$, neutral saddle-focus ($\psi_4 = 0$);
4. at $(\alpha, \beta) = (6.00000, 7.191375)$, neutrally-divergent saddle-focus ($\psi_5 = 0$).

The transition from tame homoclinic orbit to chaotic occurs at the neutral saddle-focus for this example, because the double real leading eigenvalue is non-determining. The degeneracies 1–4 above occur when the homoclinic locus crosses certain codim 1 loci corresponding to the relevant degenerate conditions on the eigenvalues. For the system (5.12), (5.13), these codim 1 loci are defined by (Khibnik, Roose & Chua 1993):

1. neutral saddle: $\beta = \frac{7}{36}\alpha(6 - \alpha)$;
2. double eigenvalue: $3\lambda^2 + 2p_1\lambda + p_2 = 0$, where $\lambda < 0$ is the double eigenvalue and $p_1 = \alpha c_3 + 1$, $p_2 = \beta + \alpha(c_3 - 1)$, $p_3 = \alpha\beta c_3$ are the coefficients of the characteristic polynomial of the Jacobian at the origin;
3. neutral saddle-focus: $2p_1^3 + p_1 p_2 + p_3 = 0$;
4. neutrally-divergent saddle-focus: $\alpha = -1/c_3$.

The numerically obtained parameter values for each of the codim 2 bifurcations can easily be seen to satisfy the appropriate condition to within 5 decimal places. Also, our parameter values agree with those obtained by Khibnik, Roose & Chua (1993) to within the number of decimal places given there (three). It should be stressed that we have obtained these parameter values directly whereas in Khibnik, Roose & Chua (1993) the loci of degenerate eigenvalues and of homoclinic orbits (obtained using shooting) were computed independently and points of intersection sought *a posteriori*.

Also depicted in fig. 5.3 are the results of the continuation of the locus of homoclinic orbits with decreasing α. The computation shown in fig. 5.3 was terminated at $(\alpha, \beta) = (0.55035, 0.47477)$, beyond which the code converged to a solution which was far from homoclinic (due to the slow convergence to the origin of the homoclinic orbit of the Bogdanov-Takens normal form). It was found that the Bogdanov-Takens point could be approached more closely by first continuing the solution in T and then computing the locus with a larger value of T.

Fig. 5.4 shows the results of three-parameter continuation of the loci of the degenerate homoclinic orbits corresponding to labels 1, 2 and 4 in fig. 5.3, with α, β and c_3 as free parameters. A codim 3 point (intersection point between the three curves) is found at

$$\alpha = 1.179320, \quad \beta = 1.02161, \quad c_3 = -0.26767,$$

corresponding to eigenvalues of the form

$$(-\lambda, -\lambda, \lambda)$$

with $\lambda = 0.685151$. Notice that only the locus of double real leading eigenvalue homoclinic orbits was computed smoothly though the codim 3 point (thus, only by computing this locus could codim 3 point be accurately detected); the other two codim 2 loci were found to *terminate* there. While the possibility of such a codim 3 homoclinic bifurcation occurring for (5.12) was conjectured in Khibnik, Roose & Chua (1993), we do not believe that it has received any theoretical treatment yet.

5.4 Electronic Circuit of Friere et al.: Hopf-Shil'nikov

Freire et al. (1993) have considered an electronic circuit that represents an autonomous electronic circuit similar to that originally proposed by Shinriki, Yamamoto & Mori (1981). The circuit is modelled by the following system of three ODEs

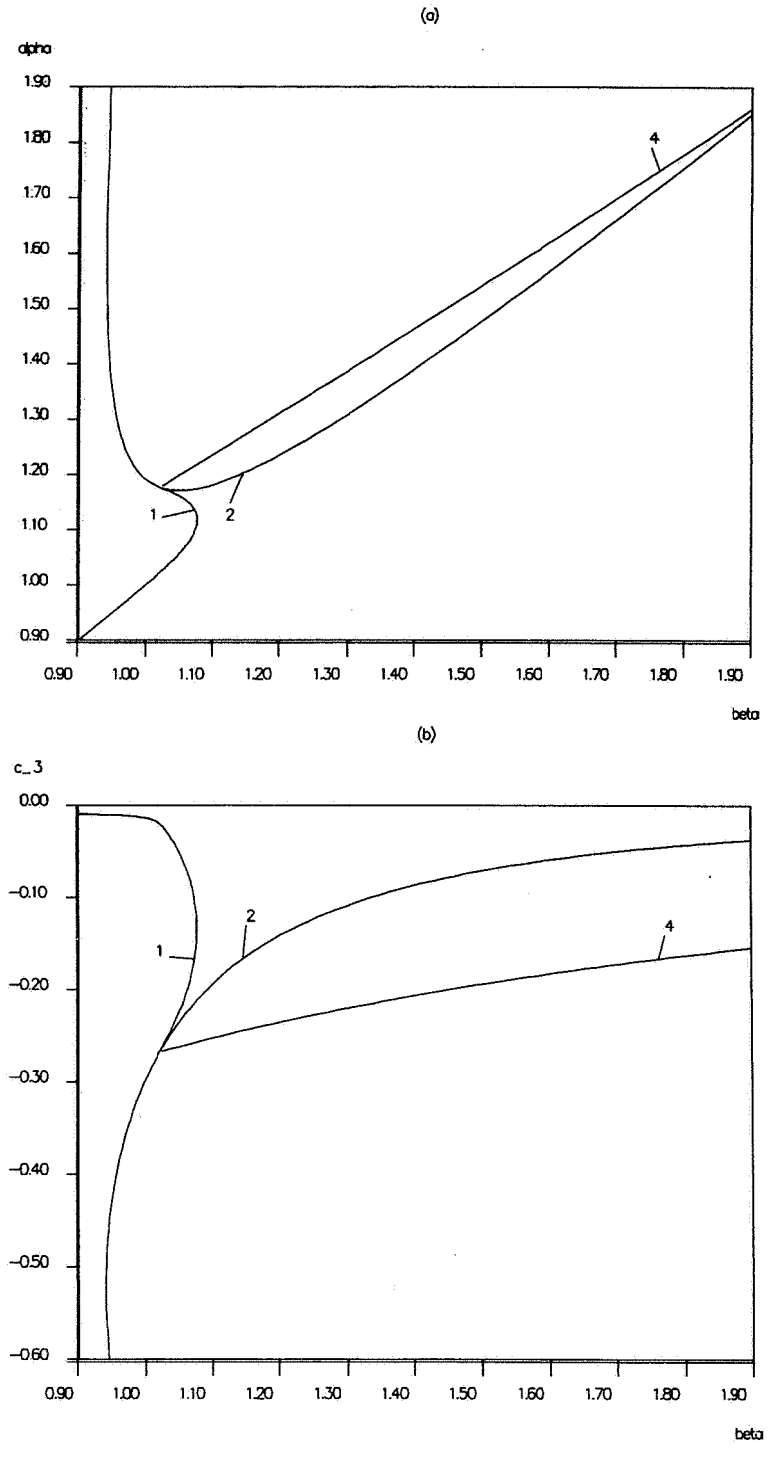

Figure 5.4: Projection of loci of degenerate homoclinic orbits onto the (α, β) and (β, c_3) planes.

$$\begin{cases} r\dot{x} &= -\nu x + \beta(y-x) - A_3 x^3 + B_3(y-x)^3, \\ \dot{y} &= -\beta(y-x) - z - B_3(y-x)^3, \\ \dot{z} &= y. \end{cases} \tag{5.14}$$

Notice that (5.14) also has odd symmetry and, at certain values of the parameters ν, β, r, A_3, B_3 "contains" the model (5.12) of Chua's circuit given that the coefficients (5.13) of the even terms in $\phi(x)$ are zero. The reader is referred to Freire et al. (1993) for more details of the model and of its dynamics. Here we focus only on loci of homoclinic orbits to the origin in the (μ, β)-plane for the fixed values

$$r = 0.6, \quad A_3 = 0.328578, \quad B_3 = 0.933578. \tag{5.15}$$

There is then a Bogdanov-Takens point at $(\nu, \beta) \approx (-0.8, 0.8)$, and the emanating locus of homoclinic orbits undergoes the same bifurcation sequence as in fig. 5.3 with the addition of a Shil'nikov-Hopf singularity occurring as the locus crosses the line $\{\beta = 0\}$ of Hopf bifurcations of the origin.

Fig. 5.5 (cf. fig. 3 in Freire et al. (1993)) shows the results of using our continuation approach on (5.14), (5.15). The same starting procedure as in sect. 5.3 was used. The parameter values we obtain for the degenerate homoclinic orbits are:

1. neutral saddle $(\psi_1 = 0)$: $(\nu, \beta) = (-0.774659, 0.774612)$;
2. double real leading eigenvalue $(\psi_2 = 0)$: $(\nu, \beta) = (-0.759057, 0.742871)$;
3. neutral saddle-focus $(\psi_4 = 0)$: $(\nu, \beta) = (-0.720398, 0.591215)$;
4. neutrally-divergent saddle-focus $(\psi_1 = 0)$: $(\nu, \beta) = (-0.725694, 0.453559)$;
5. Shil'nikov-Hopf $(\psi_9 = 0)$: $(\nu, \beta) = (-1.026478, -3.3 \times 10^{-11})$.

Notice from fig. 5.5(a) that the code computes a locus passing through the Shil'nikov-Hopf point and thus is able to detect the singularity accurately. Observe from fig. 5.5(b) that the orbit on the locus on the "far" side of the Shil'nikov-Hopf homoclinic orbit is a "point-to-periodic" heteroclinic connection, as predicted in section 4 above.

5.5 The Shimizu-Morioka Equations: Inclination Switch

We now turn to an example for which inclination switching is known to occur. The following system of equations

$$\begin{cases} \dot{x} &= y \\ \dot{y} &= \kappa y - \lambda x - xz \\ \dot{z} &= -z + x^2 \end{cases} \tag{5.16}$$

were considered by Rucklidge (1993) as a model of convection in a vertical magnetic field, in the limit of tall, thin rolls. They may be obtained by a scaling of co-ordinates from the simplified model of the Lorenz equations derived by Shimizu & Morioka (1980), and analysed by A. Shil'nikov (1991, 1993). At $\alpha = \lambda = 0$ there is a Bogdanov-Takens singularity and a locus of (a pair of symmetry-related) homoclinic orbits to the origin emanates into the third quadrant in the (κ, λ)-plane. Loci of homoclinic orbits described by these two parameters have been computed by Shil'nikov and Rucklidge using shooting and long-period periodic orbits respectively. In fact there are many interesting codim 2 homoclinic bifurcations in this model, including a Bykov heteroclinic loop to a saddle-focus, which (due to the symmetry $x \to -x, y \to -y, z \to z$) have consequences for the existence of Lorenz-like strange attractors. The reader is referred to Rucklidge (1993) and Shil'nikov (1993) for a complete account, here we focus only on the simplest few homoclinic bifurcations.

Fig. 5.6 shows loci of two distinct (symmetry-related pairs of) homoclinic orbits. For all the relevant parameter values the origin has a one-dimensional unstable manifold. Due to the invariance of the z-axis of (5.16), the origin is always a saddle and, therefore, we also solve the normalised adjoint variational equations (4.5) to compute the orientation. Both loci were started using shooting at estimations for parameter values obtained from Rucklidge (1993), the solutions of (4.5) computed

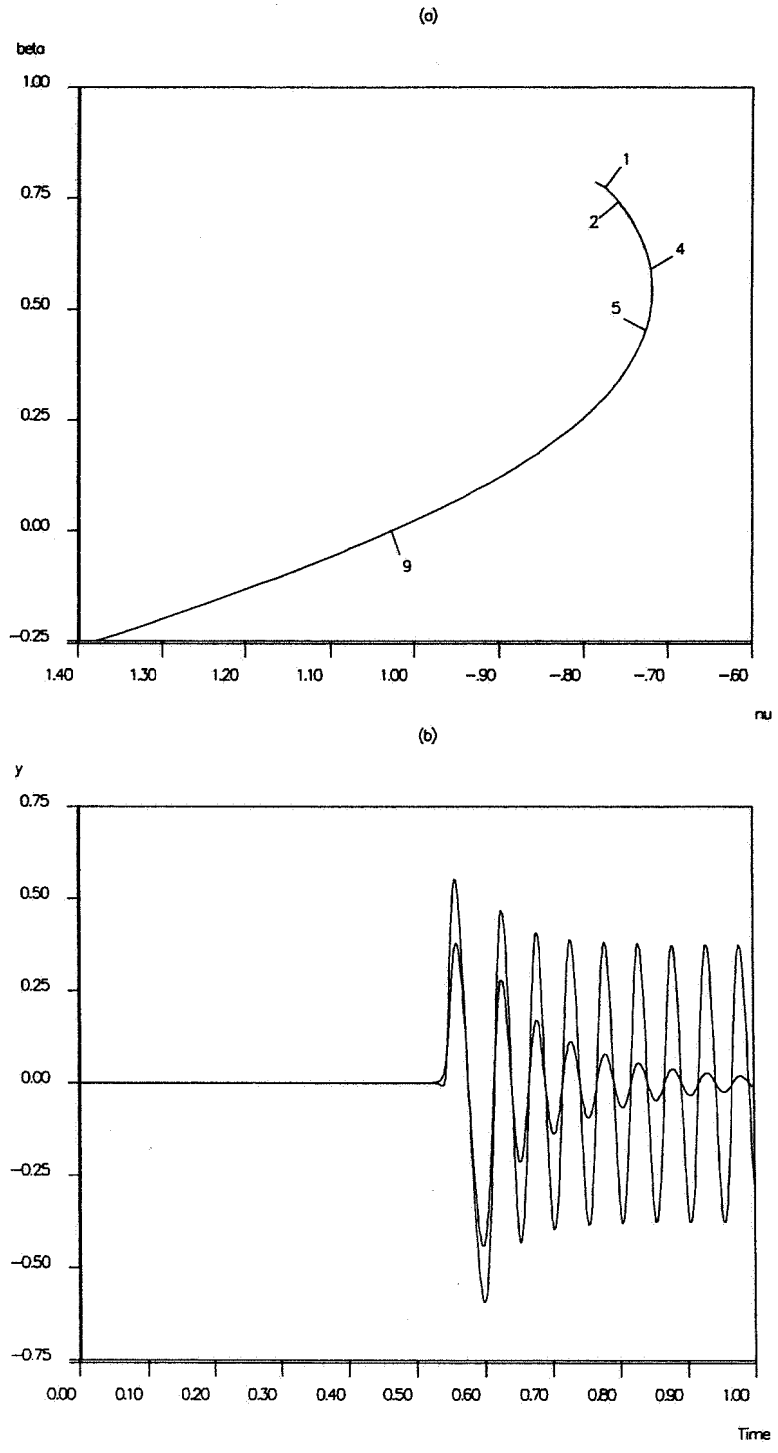

Figure 5.5: (a) Locus of homoclinic orbit in Freire *et al.*'s circuit; labels are the indices of the test functions that are zeroed. (b) Graphs of the computed orbits at $\beta = -0.1, 0.1$, where the time-interval is normalised to unity.

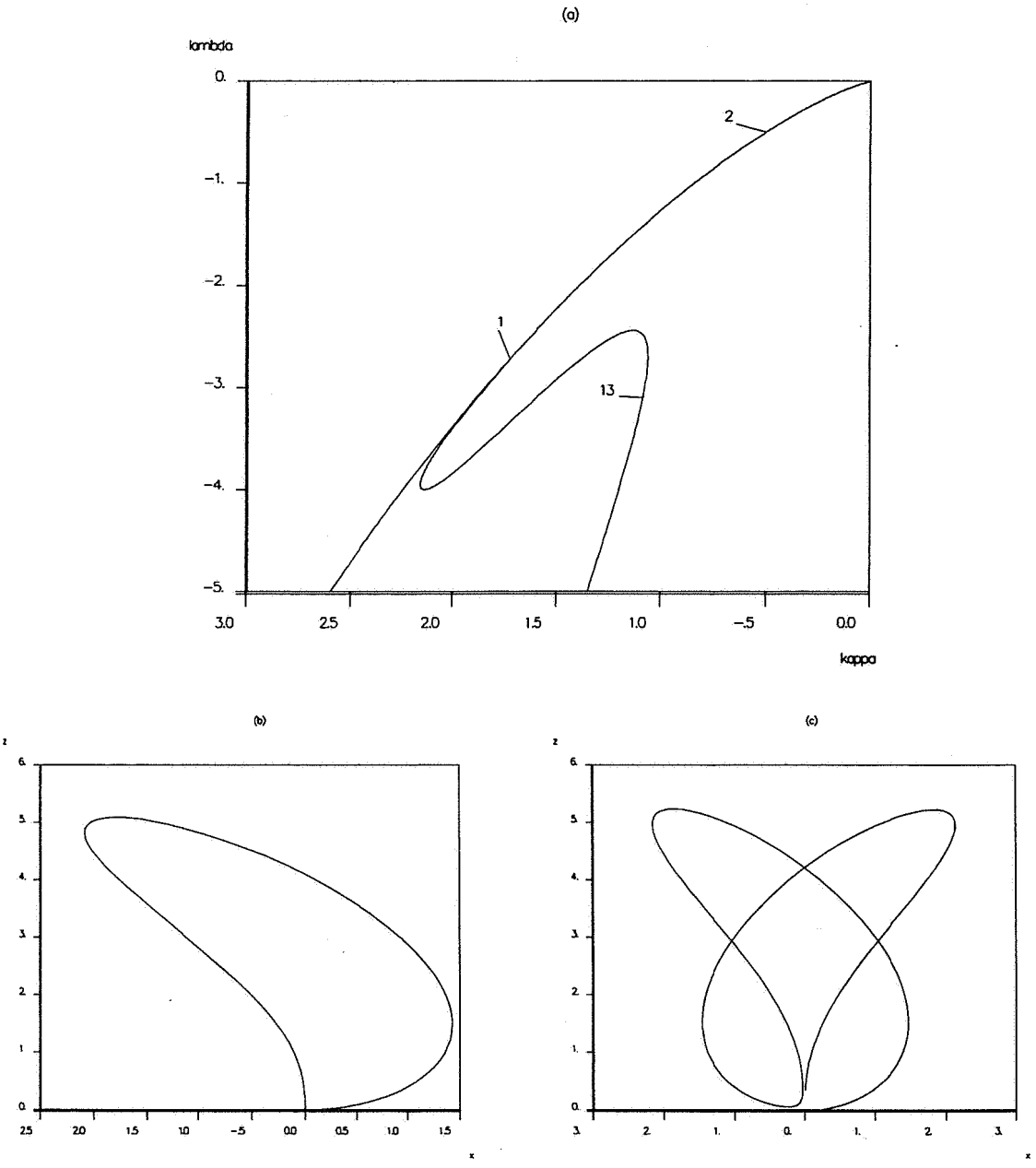

Figure 5.6: (a) Loci of homoclinic orbits in the Shimizu-Morioka equations. (b),(c) Primary and double homoclinic orbits near 1.

once the shooting procedure had converged. The branch containing labels 1 and 2 in fig. 5.6(a) is the locus of "primary" homoclinic orbits that emanate from the origin of (κ, λ)-plane. At the point labelled 2, $(\kappa, \lambda) \approx (-0.500, -0.500)$, there are double non-determining real eigenvalues. However, this bifurcation is non-generic due to the invariance of the z-axis; the pair of coalescent eigenvalues do not become complex, but merely cross each other on the real axis. The consequences of this bifurcation are that the symmetric pair of homoclinic orbits switch from a "figure-of-eight" to a "butterfly" configuration, both of which are tame (see Rucklidge (1993) for more details on this bifurcation). We found that our code was unable to continue a locus of homoclinic orbits through this bifurcation point; instead we had to compute the locus in two pieces, using two separate starting solutions, and computing towards the bifurcation from both sides.

At label 1 in fig. 5.6(a), $(\kappa, \lambda) = (-1.724323, -2.724323)$, there are resonant real eigenvalues which gives rise to a form of resonant homoclinic doubling. Beyond this bifurcation the primary homoclinic orbit is chaotic, causing the birth of a Lorenz-attractor. The second locus depicted in fig. 5.6(a) is that of the double homoclinic orbit that is born at 1. Figs. 5.6(b),(c) depict the primary and doubled orbits in a neighbourhood of this codim 2 point. Both orbits are non-twisted at this point.

At label 13, $(\kappa, \lambda) = (-1.087756, -3.101548)$, there is an inclination-switch bifurcation of the branch of double homoclinic orbits. Due to the symmetry, the bifurcation is non-generic here and the codim 2 point causes a "side-switching" of the bifurcation to Lorenz attractors in addition to extra loci of period-doubling bifurcations (Rucklidge 1993, Shil'nikov 1993). Fig. 5.7(a) shows the homoclinic orbit at the inclination switch (note that, away from point 1, the homoclinic orbit is no longer approximately "double" the primary one), and Fig. 5.7(b) shows the first component of the solution (4.5),(4.10),(4.11) at the bifurcation and at two points on either side of it on the homoclinic locus (at $\kappa = -3.013862$, -3.101548 and -3.101780). Note that the right-hand end points of these solutions are virtually the same (≈ 0.3864, the first component of w_1^*) whereas the left-hand end point switches between $\approx \pm 0.6099$, the first component of v_1^*. Note that at the critically-twisted point, the first component of the left-hand end point is zero (because v_2^* lies on the z-axis). These observations from fig. 5.7(b) all accord with the theory of the inclination switch bifurcation and provide independent corroboration that the code has accurately detected an inclination switch.

Note that the parameter values we obtain for the inclination switch differ from those obtained by Rucklidge (1993) in the third decimal place (Rucklidge gives these values only to 3 D.P.). We have re-computed the branch of doubled homoclinic orbits, computing the orientation via the tangent space to the stable manifold (i.e. solutions of the normalised variational equations, see Kuznetsov (1991)) and found the parameter values of the inclination switch to agree with those given above to 6 D.P. We remark that the inclination switch in this example was previously found using a shooting technique that is unique to equations with a one-dimensional unstable manifold and $\mathbb{Z}_2$-symmetry; namely monitoring the *code change* of the unstable manifold as the homoclinic manifold $\mathcal{H}_i$ is crossed (Sparrow 1982, Glendinning 1989*a*). In contrast we have located an inclination switch directly, using a method which, in principle, can work for arbitrary systems.

6. Concluding Remarks

In this paper we have presented a numerical method to locate and continue a number of codim 2 homoclinic bifurcations. The list of supported codim 2 bifurcations covers all known global codim 2 cases in which only a unique homoclinic orbit to a hyperbolic equilibrium is involved.

The continuation of several other codim 2 bifurcations at which *two* orbits are present that are homoclinic to the same hyperbolic equilibrium could easily be incorporated into our scheme, as well as certain codim 2 cases of *heteroclinic cycles* connecting two hyperbolic equilibria. In all these cases the equations and boundary conditions for both homo/hetero-clinic orbits can be set independently. However, the problem of starting solutions seems to be more difficult for these cases, since a test function to detect such a singularity while continuing a branch of primary homoclinic orbits cannot be expressed in terms of quantities associated with the primary orbit alone. The situation is particularly involved for the heteroclinic cases due to the formal non-existence of a homoclinic orbit at the critical parameter values. One possible way of overcoming this difficulty is to follow a heteroclinic branch and monitor the possible appearance of another heteroclinic orbit. Alternatively, in low dimensions, one can rely upon interactive visualisation of the invariant manifolds, using *dstool* (Back, Guckenheimer,

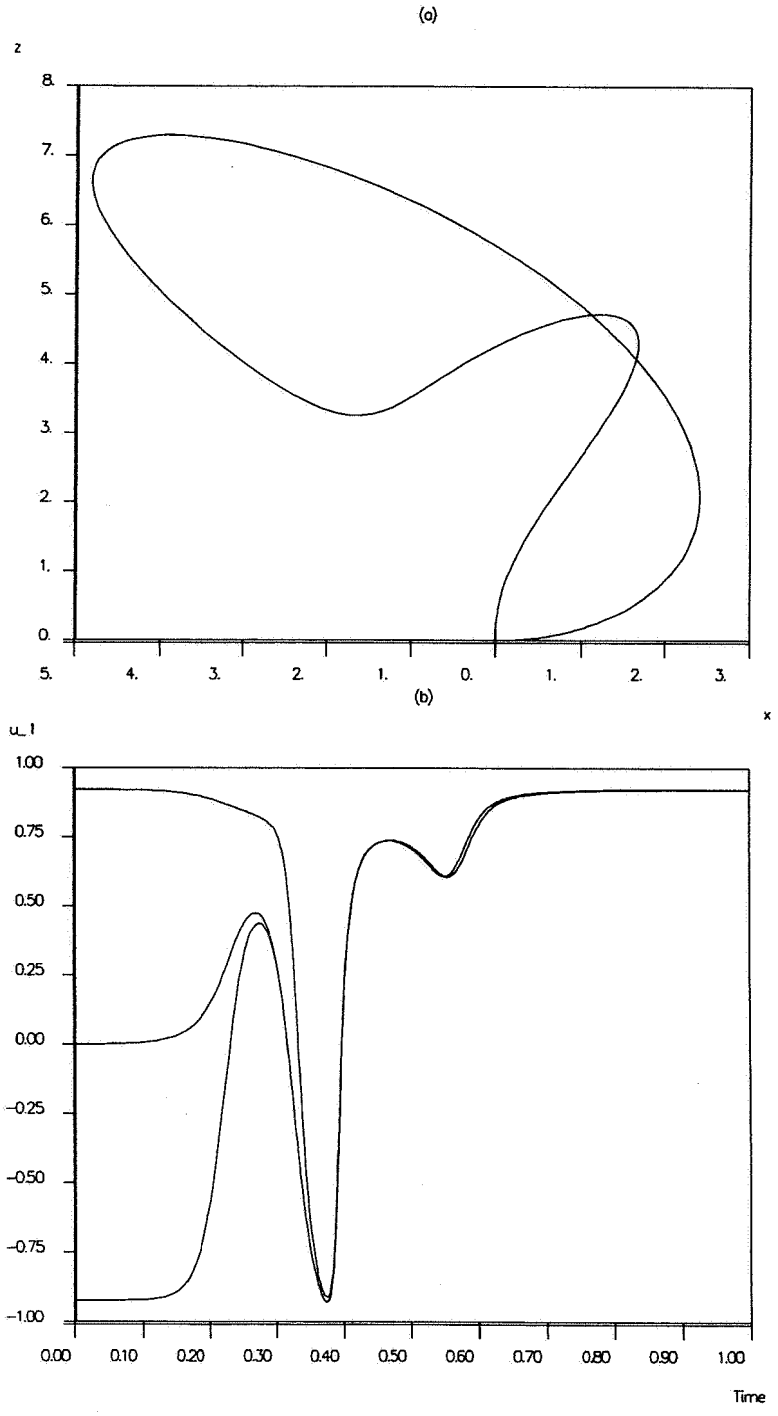

Figure 5.7: (a) Critically twisted homoclinic orbit. (b) Behaviour of the first component of the normal vector to the stable manifold of the homoclinic obit upon crossing the inclination switch.

Myers & Worfolk 1992) for example, to detect the bifurcations in question.

The method we present has no difficulties in the detection and continuation of a Shil'nikov-Hopf bifurcation at which there is a homoclinic orbit to a non-hyperbolic saddle-focus. For a saddle-node homoclinic orbit, however, it cannot be used. As it has been pointed out, a special technique based on non-linear approximations of the invariant manifolds of the saddle-node (Schecter 1993*a*, Friedman 1993, Friedman & Doedel 1993) has proved to be useful here.

Another area we have not covered is codim 2 homcolinic bifurcations that are unique to systems with certain symmetries (e.g. the bifurcation in the Shimizu-Morioka equations that occurs at label 2 in fig. 5.6(a)). In order to deal with homoclinic bifurcations with symmetry in a systematic way one would have to consider each symmetry independently, in much the same way as one does for local bifurcations with symmetry, and to derive test functions and continuation techniques for the codim two homoclinic orbits that occur generically a two-parameter system with such a symmetry.

The detection of codimension-two homoclinic orbits, as studied in this paper, is only the first stage in a complete numerical framework for the study of homoclinic bifurcations. When a codim 2 homoclinic bifurcation is located on a plane described by two free parameters, an important problem is to *analyse* the bifurcation, that is to determine which of the parametric portraits is present in the particular system and to find local approximations for the codim 1 bifurcation curves existing nearby. For the three systems mentioned in the introduction, for example, one would like to be able to automatically compute the boundary of the horn of chaotic dynamics that emanates from each of the codim 2 homoclinic points in question. To do this one requires the software to compute asymptotic approximations for the codim 1 bifurcation loci that emanate from the codim 2 point and then to "switch branches" to follow these loci in 2 parameters (in much the same way as codes such as AUTO and LOCBIF (Khibnik, Kuznetsov, Levitin & Nikolaev 1993) deal with codim 0 loci of solutions emanating from a codim 1 bifurcation of equilibria or periodic orbits).

The problem of finding local approximations to bifurcating branches is non-trivial, however, for homoclinic bifurcations even if there is only finite number of bifurcation curves for nearby parameter values (like in the resonant saddle case). In many cases, curves originating at the codim 2 point have an *infinite order* tangency with the primary homoclinic curve (the two loci are *exponentially close* there) and, thus, their Taylor approximations do not help. In these cases, more accurate exponential asymptotic expansions should be used. Note that none of the available asymptotics are detailed enough to be implemented numerically, *i.e.* it is not clear how to compute the constants in these asymptotic expressions. The problem becomes even more difficult if there is an infinite number of codim 1 curves emanating from the codim 2 point, each with an infinite-order tangency to the primary homoclinic branch. The double homoclinic curves in Belyakov's double leading eigenvalue case, for example, have such a tangency and the phase-space difference between these orbits can be defined only in non-invariant terms which depend on the closeness to the codim 2 point. However, whereas these orbits are close in phase space, they are not close as functions of time and it may be possible to use the known properties of the orbits to create good starting guesses for a shooting approach. Once the orbits have been thus located, they can be followed (both towards and away from the codim 2 point) using the method outlined in section 3, because all double homoclinic orbits are bounded away from each other in the norm used in Theorem 3.1. Such an approach was used in Champneys & Toland (1993) to systematically locate and follow an infinite family of double homoclinic orbits in a reversible system.

Another practically important issue is the derivation of the asymptotic formulae for the homoclinic and heteroclinic bifurcation curves starting at *local* codim 2 bifurcation points. This problem has been solved for the Bogdanov-Takens bifurcation by Beyn (1991) and can be considered as a part of a wider program to derive computational formulae for global bifurcation manifolds arising from local multi-codimension bifurcations. See also Gaspard (1993) where a locus of saddle-focus homoclinic orbits emanating from a Gavrilov-Guckenheimer point is computed.

We recognize that the AUTO driver we have written for the continuation of codim 2 homoclinic bifurcations can be considered only as a short-term intermediate answer to the needs of applications. First of all, it supports only a limited number of codim 2 bifurcations (see above). The most serious drawback, however, is its non-interactive nature. The importance of homoclinic bifurcations to the understanding of dynamical behaviour arising from a wide number of fields has already been remarked,

and interactivity is of key importance if a code is to be used as a tool by the wider scientific community. An integrated interactive system incorporating various starting procedures and continuation methods has yet to be developed.

Finally, let us point out that there are still codim 2 homoclinic bifurcations that have not yet been analysed theoretically (like three leading eigenvalues) or which have so-far received an incomplete analysis only. Some of the cases which were originally studied more than a decade ago may now be more tractable using modern techniques such as finite-smooth normalization. Another challenge to both pure and applied mathematicians is the absence of sound example systems exhibiting certain of the codim 2 bifurcations we have reviewed, notably the orbit switch bifurcation.

In conclusion, we believe that these are the early days of numerical homoclinic bifurcation analysis and there remains much to be done. We hope the present work will be of some interest to both the pure and applied bifurcation communities and will stimulate the necessary interaction between them for progress to be made.

REFERENCES

Afraimovich, V., Arnold, V., Il'yashenko, Y. & Šil'nikov, L. (1993), Theory of Bifurcations, *in* V. Arnold, ed., 'Dynamical Systems, 5. Encyclopaedia of Mathematical Sciences', Springer-Verlag, New York.

Amick, C. & Toland, J. (1992), 'Homoclinic orbits in the dynamic phase space analogy of an elastic strut', *European J. Appl. Maths.* **3**, 97–114.

Andronov, A. & Leontovich, E. (1939), 'Some cases of the dependence of the limit cycles upon parameters', *Uch. Zap. Gork. Univ.* **6**, 3–24. in Russian.

Andronov, A., Leontovich, E., Gordon, I. & Maier, A. (1971), *Theory of Bifurcations of Dynamical Systems on a Plane*, Israel Program of Scientific Translations, Jerusalem.

Arnéodo, A., Coullet, P. & Tresser, C. (1982), 'Oscillators with chaotic behavior: An illustration of a theorem by Shil'nikov', *J. Stat. Phys.* **27**, 171–182.

Arniéodo, A., Argoul, F., Elezgaray, J. & Richetti, P. (1993), 'Homoclinic chaos in chemical systems', *Physica D* **62**, 134–169.

Back, A., Guckenheimer, J., Myers, M. & Worfolk, P. (1992), *dstool; Dynamical Systems Toolkit with Interactive Graphic interface User's Manual*, Cornell University.

Belyakov, L. (1974), 'A case of the generation of a periodic motion with homoclinic curves', *Mat. Zam.* **15**, 336–341.

Belyakov, L. (1980), 'The bifurcation set in a system with a homoclinic saddle curve', *Mat. Zam.* **28**, 910–916.

Belyakov, L. (1984), 'Bifurcation of systems with homoclinic curve of a saddle-focus with saddle quantity zero', *Mat. Zam.* **36**, 838–843.

Belyakov, L. & Shil'nikov, L. (1990), 'Homoclinic curves and complex solitary waves', *Selecta Mathematica Sovietica* **9**, 219–228.

Beyn, W.-J. (1990*a*), Global bifurcations and their numerical computation, *in* D. Roose, A. Spence & B. De Dier, eds, 'Continuation and Bifurcations: Numerical Techniques and Applications', Kluwer, Dordrecht, Netherlands, pp. 169–181.

Beyn, W.-J. (1990*b*), 'The numerical computation of connecting orbits in dynamical systems', IMA *J. Num. Anal.* **9**, 379–405.

Beyn, W.-J. (1991), Numerical Methods for Dynamical Systems, *in* W. Light, ed., 'Advances in Numerical Analysis, Volume I, Nonlinear Partial Differential Equations and Dynamical Systems', Oxford University Press, pp. 175–236.

Budd, C. (1989), 'Applications of Shilnikov's theory to semilinear elliptic equations', SIAM *J. Math. Anal.* **20**, 1069–1080.

Bykov, V. (1977), 'On the birth of periodic motions from a separatrix contour of a three-dimensional system', *Uspekhi Mat. Nauk* **32(6)**, 213–214. in Russian.

Bykov, V. (1980), Bifurcations of dynamical systems close to systems with a seperatrix contour containing a saddle-focus, *in* E. Leontovich Andronova, ed., 'Methods of the Qualitative Theory of Differential Equations', Gor'kov. Gos. Univ., Gorki, pp. 44–72. In Russian.

Bykov, V. (1993), 'The bifurcations of separatrix contours and chaos', *Physica D* **62**, 290–299.

Champneys, A. (1993), 'Homoclinic tangencies in the dynamics of articulated pipes conveying fluid', *Physica D.* **62**, 347–359.

Champneys, A. & Spence, A. (1993), 'Hunting for homoclinic orbits in reversible systems: a shooting technique', *Adv. Comp. Math.* **1**, 81–108.

Champneys, A. & Toland, J. (1993), 'Bifurcation of a plethora of multi-modal homoclinic orbits for autonomous Hamiltonian systems', *Nonlinearity* **6**, In press.

Chow, S., Deng, B. & Terman, D. (1990), 'The bifurcations of homoclinic and periodic orbits from two heteroclinic orbits', SIAM *J. Math. Anal.* **21**, 179–204.

Chow, S.-N. & Lin, X.-B. (1990), 'Bifurcation of a homoclinic orbit with a saddle-node equilibrium', *J. Diff. Int. Eqs.* **3**, 319–349.

Chow, S.-N., Deng, B. & Fiedler, B. (1990), 'Homoclinic bifurcation at resonant eigenvalues', *J. Dyn. Diff. Eqs.* **2**, 177–244.

Deng, B. (1989), 'The Shil'nikov problem, exponential expansion, strong λ-lemma, C^1-linearization, and homoclinic bifurcation', *J. Diff. Eqs.* **79**, 189–231.

Deng, B. (1990), 'Homoclinic bifurcations with nonhyperbolic equilibria', SIAM *J. Math. Anal.* **21**, 693–720.

Deng, B. (1991), Constructing homoclinic orbits and chaos, Department of Mathematics and Statistics, University of Nebraska-Lincoln.

Deng, B. (1993), 'Homoclinic twisting bifurcations and cusp horseshoe maps', *J. Dyn. Diff. Eqs.*

Doedel, E. (1981), 'AUTO, a program for the automatic bifurcation analysis of autonomous systems', *Cong. Numer.* **30**, 265–384.

Doedel, E. & Friedman, M. (1989), 'Numerical computation of heteroclinic orbits', *J. Comp. Appl. Math.* **26**, 159–170.

Doedel, E. & Kernévez, J. (1986), AUTO: Software for continuation problems in ordinary differential equations with applications, Technical report, California Institute of Technology. Applied Mathematics.

Doedel, E., Keller, H. & Kernévez, J. (1991*a*), 'Numerical analysis and control of bifurcation problems: (I) Bifurcation in finite dimensions', *Int. J. Bifurcation and Chaos* **1**, 493–520.

Doedel, E., Keller, H. & Kernévez, J. (1991*b*), 'Numerical analysis and control of bifurcation problems: (II) Bifurcation in infinite dimensions', *Int. J. Bifurcation and Chaos* **1**, 745–772.

Evans, J., Fenichel, N. & Feroe, J. (1982), 'Double impulse solutions in nerve axon equations', SIAM *J. Appl. Math.* **42**, 219–234.

Feroe, J. (1981), 'Travelling waves of infinitely many pulses in nerve equations', *Math. Biosci.* **55**, 189–204.

Feroe, J. (1986), 'Existence of travelling wave trains in nerve axon equations', SIAM *J. Appl. Math.* **45**, 1079–1097.

Fiedler, B. (1992), Global pathfollowing of homoclinic orbits in two-parameter flows, Technical report, Institut für Angewandte Analysis und Stochastik, Berlin. Applied Mathematics.

Fife, P. (1978), 'Asymptotic states for equations of reaction and diffusion', *Bull. Amer. Math. Soc.* **84**, 693–724.

FitziHugh, R. (1961), 'Impulses and physiological states in theoretical models of nerve membrane',

Biophys. J. **1**, 445–446.

Freire, E., Rodríguez-Luis, A. & Ponce, E. (1993), 'A case study for homoclinic chaos in an autonomous electronic circuit: A trip from takens-bogdanov to hopf-shilnikov', *Physica D* **62**, 230–253.

Friedman, M. (1993), 'Numerical analysis and accurate computation of heteroclinic orbits in the case of center manifolds.', *J. Dyn. Diff. Eqs* **5**, 59–87.

Friedman, M. & Doedel, E. (1991), 'Numerical computation of invariant manifolds connecting fixed points', SIAM *J. Numer. Anal.* **28**, 789–808.

Friedman, M. & Doedel, E. (1993), 'Computational methods for global analysis of homoclinic and heteroclinic orbits: A case study', *J. Dyn. Diff. Eqs.* **5**, 37–57.

Friedman, M., Doedel, E. & Monteiro, A. (1993), On locating homoclinic and heteroclinic orbits, Technical report, Cornell Theroy Center; Center for Applied Mathematics, Cornell University.

Gambaudo, J. (1987), Ordre, désordre, et frontière des systémes Morse-Smale, PhD thesis, Université de Nice.

Gambaudo, J., Glendinning, P. & Tresser, C. (1985), 'Stable cycles with complicated structure', *J. de Phys. Lettre* **46**, L:633–657.

Gaspard, P. (1983), 'Generation of a countable set of homoclinic flows through bifurcation', *Phys. Lett.* A **97**, 1–4.

Gaspard, P. (1987), Tangences Homoclinies dans les Systemes Dynamiques Dissipatifs, PhD thesis, Université Libre de Bruxelles.

Gaspard, P. (1993), 'Local birth of homoclinic chaos', *Physica D* **62**, 94–122.

Gaspard, P. & Wang, X.-J. (1987), 'Homoclinic orbits and mixed-mode oscillations in far-from-equilibrium systems', *J. Stat. Phys.* **48**, 151–199.

Gaspard, P., Arnéodo, A., Kapral, R. & Sparrow, C., eds (1993), *Homoclinic Chaos, Physica D.* **62** (1-4), special issue.

Gaspard, P., Kapral, R. & Nicolis, G. (1984), 'Bifurcation phenomena near homoclinic systems: a two- parameter analysis', *J. Stat. Phys.* **35**, 687–727.

Gavrilov, N. & Silnikov, L. (1972), 'On three-dimensional systems close to systems with a structurally unstable homoclinic curve: I', *Mat.* USSR *Sb.* **17**, 467–485.

Gavrilov, N. & Silnikov, L. (1973), 'On three-dimensional systems close to systems with a structurally unstable homoclinic curve: II', *Mat.* USSR *Sb.* **19**, 139–156.

Glendinning, P. (1988), Global bifurcations in flows, *in* T. Bedford & J. Swift, eds, 'New Directions Dynamical Systems', C.U.P.

Glendinning, P. (1989*a*), 'Global structures of bifurcations: a combinatorial approach', *Phys. Lett. A.* **141**, 391–396.

Glendinning, P. (1989*b*), 'Subsidiary bifurcations near bifocal homoclinic orbits', *Math. Proc. Camb. Phil. Soc.* **105**, 597–605.

Glendinning, P. & Sparrow, C. (1984), 'Local and global behaviour near homoclinic orbits', *J. Stat. Phys.* **35**, 645–696.

Gruewdler, J. (1992), 'Homoclinic solutions of autonomous dynamical systems in arbitrary dimensions', SIAM *J. Math. Anal.* **23**, 702–722.

Guckenheimer, J. & Holmes, P. (1983), *Nonlinear Oscillations, Dynamical Systems and Bifurcations of Vector Fields*, Springer-Verlag, New York, USA.

Hassard, B. (1980), Computation of invariant manifolds, *in* P. Holmes, ed., 'New Approaches to Nonlinear Problems in Dynamics', SIAM, pp. 27–42.

Hastings, S. (1976), 'On the existence of homoclinic and periodic orbits for the fitzhugh-nagumo equations', *Quart. J. Math. (Oxford)* **27**, 123–134.

Hastings, S. (1982), 'Single and multiple pulse waves for the fitzhugh-nagumo equations', SIAM *J. Appl. Math.* **42**, 247–260.

Healey, J., Broomhead, D., Cliffe, K., Jones, R. & Mullin, T. (1991), 'The origins of chaos in a modified Van der Pol Oscillator', *Physica D* **48**, 322–339.

Hirsch, M., Pugh, C. & Shub, M. (1977), *Invariant Manifolds*, Springer-Verlag, Berlin.

Hirshcberg, P. & Knobloch, E. (1993), 'Šil'nikov-Hopf bifurcation', *Physica D* **62**, 202–216.

Hofer, H. & Wysocki, K. (1990), 'First order elliptic systems and the existence of homoclinic orbits in Hamiltonian systems', *Math. Annalen* **288**, 483–503.

Homberg, A., Kokubu, H. & Krupa, M. (1993), The cusp horseshoe and its bifurcations in the unfolding of an inclination-flip homoclinic orbit, Technical report, Department of Mathematics, University of Groningen.

Jones, C. (1984), 'Stability of the travelling wave solution of the FitzHugh-Nagumo system', *Trans. Amer. Math. Soc.* **286**, 431–469.

Jones, C., Koppel, N. & Langer, R. (1991), Construction of the FitzHugh-Nagumo pulse using differential forms, *in* H. Swinney, G. Aris & D. Aronson, eds, 'Patterns and Dynamics in Reactive Media. IMA Volumes in Mathematics and its Applications, **37**', Springer-Verlag, New York, pp. 101–115.

Khibnik, A., Kuznetsov, Y., Levitin, V. & Nikolaev, E. (1993), 'Continuation techniques and interactive software for bifurcation analysis of ODEs and iterated maps', *Physica D* **62**, 360–371.

Khibnik, A., Roose, D. & Chua, L. (1993), On periodic orbits and homoclinic bifurcations in chua's circuit with smooth nonlinearity, Preprint: Katholieke Universiteit Leuven, Belgium.

Kirchgassner, K. (1988), 'Nonlinearly Resonant Surface Waves and Homoclinc Bifurcation', *Adv. Appl. Mech.* **26**, 135–181.

Kisaka, M., Kokubu, H. & Oka, H. (1993*a*), 'Bifurcation to n-homoclinic orbits and n-periodic orbits in vector fields', *J. Dyn. Diff. Eqs.* In press.

Kisaka, M., Kokubu, H. & Oka, H. (1993*b*), Supplement to homoclinic doubling bifurcation in vector fields, *in* R. Bamon, J. Labarca, J. Lewowicz & J. Palis, eds, 'Dynamical Systems', Longman, pp. 92–116.

Kuznetsov, Y. (1982), Existence and stability of the travelling waves in reaction-diffusion systems with one space variable, Reseach Computing Centre, USSR Academy of Sciences, Pushchino. In Russian.

Kuznetsov, Y. (1983), One-dimensional invariant manifolds in ordinary differential equations depending upon parameters. FORTRAN Software Series, 8, Research Computing Centre, USSR Academy of Sciences, Pushchino. In Russian.

Kuznetsov, Y. (1990), Computation of invariant manifold bifurcations, *in* D. Roose, A. Spence & B. De Dier, eds, 'Continuation and Bifurcations: Numerical Techniques and Applications', Kluwer, Dordrecht, Netherlands, pp. 183–195.

Kuznetsov, Y. (1991), 'Numerical analysis of the orientability of homoclinic trajectories', *Int. Ser. Numer. Math.* **97**, 237–241.

Kuznetsov, Y. & Panfilov, A. (1981), Stochastic waves in the FitzHugh-Nagumo system, Technical report, Reseach Computing Centre, USSR Academy of Sciences, Pushchino. In Russian.

Kuznetsov, Y., Muratori, S. & Rinaldi, S. (1991), Homoclinic bifurcations in slow-fast second order systems, Technical report, Dipartimento di Elettronica, Politecnico di Milano.

Lin, X.-B. (1990), 'Using Melnikov's method to solve Silnikov's problems', *Proc. Royal Soc. Edinburgh* **116A**, 295–325.

Lorenz, E. (1963), 'Deterministic non-periodic flow', *J. Atmos. Sci.* **20**, 130–141.

Lukyanov, V. (1982), 'Bifurcations of dynamical systems with a saddle-point separatrix loop', *Differential. Eq.* **18**, 1049–1059.

Matsumoto, T., Chua, L. & Kumuro, M. (1985), 'The double scroll', IEEE *Trans. Circuits and Systems* **32**, 798–818.

Miura, R. (1982), 'Accurate computation of the stable solitary wave for the FitzHugh-Nagumo equations', *J. Math. Biol.* **13**, 247–269.

Nagumo, J., Arimoto, S. & Yoshizawa, S. (1962), 'An active pulse transmission line simulating nerve axon', *Proc.* IRE **50**, 2061–2070.

Nozdrachova, V. (1982), 'Bifurcation of a noncourse seperatrix loop', *Differential Eq.* **18**, 1098–1104.

Reyn, J. (1980), 'Generation of limit cycles from separatrix polygons in the phase plane', *Lect. Notes Math.* **810**, 264–289.

Rodríguez-Luis, A., Freire, E. & Ponce, E. (1990), A method for homoclinic and heteroclinic continuation in two and three dimensions, *in* D. Roose, A. Spence & B. De Dier, eds, 'Continuation and Bifurcations: Numerical Techniques and Applications', Kluwer, Dordrecht, Netherlands, pp. 197–210.

Rucklidge, A. (1993), 'Chaos in a low-order model of magnetoconvection', *Physica D.* **62**, 323–337.

Sandstede, B. (1993), Verzweigungstheorie homokliner Verdopplungen, PhD thesis, Institut fur Angewandte Analysis und Stochastik, Berlin.

Schecter, S. (1993*a*), 'Numerical computation of saddle-node homoclinic bifurcation points', SIAM *J. Num. Anal.* To appear.

Schecter, S. (1993*b*), Rate of convergence of numerical approximations to homoclinic bifurcation points, North Carolina State University.

Seydel, R. (1988), *From Equilibrium to Chaos. Practical Bifurcation and Stability Analysis*, Elsevier, New York.

Seydel, R. (1991), 'Tutorial on continuation', *Int. J. Bifurcation and Chaos* **1**, 3–11.

Shashkov, M. (1992), 'On bifurcations of separatrix contours with two saddles', *Int. J. Bifurcation and Chaos* **2**, 911–915.

Shil'nikov, A. (1991), 'Bifurcations and chaos in the morioka-shimizu system', *Selecta Mathematica Sovietica* **10**, 105–117.

Shil'nikov, A. (1993), 'On bifurcations of the Lorenz attractor in the Shimzu-Morioka model', *Physica D* **62**, 338–346.

Shil'nikov, L. (1968), 'On the generation of periodic motion from trajectories doubly asymptotic to an equilibrium state of saddle type', *Mat.* USSR *Sb.* **6**, 427–437.

Shil'nikov, L. (1969), 'On a new type of bifurcation of multidimensional dynamical systems', *Sov. Math. Dokl.* **10**, 1368–1371.

Shil'nikov, L. (1970), 'A contribution to the problem of the structure of an extended neighborhood of a rough equilibrium state of saddle-focus type', *Mat.* USSR *Sb.* **10**, 91–102.

Shimizu, T. & Morioka, N. (1980), 'On the bifurcation of a symmetric limit cycle to an asymmetric one in a simple model', *Phys. Lett. A* **76**, 201.

Shinriki, R., Yamamoto, M. & Mori, S. (1981), 'Multimode oscillations in a modified Van der Pol oscillator containing a positive nonlinear conductance', IEEE *Proc.* **69**, 394.

Smale, S. (1967), 'Differentiable dynamical systems', *Bull. Amer. Math. Soc.* **73**, 747–817.

Sparrow, C. (1982), *Lorenz Equations : Bifurcations, Chaos, and Strange Attractors*, Springer-Verlag, New York, USA.

Szmolyan, P. (1991), 'Transversal heteroclinic and homoclinic orbits in singular perturbed problems', *J. Diff. Eqs.* **92**, 252–281.

Terman, D. (1992), 'The transition from bursting to continuous spiking in excitable membrane models', *J. Nonlinear Sci.* **2**, 135–182.

Tresser, C. (1984), 'About some theorems by L.P.Sil'nikov', *Ann. Inst. Henri Poincare* **40**, 441–461.

Turaev, D. (1988), 'On the bifurcations of a homoclinic 'figure eight' of a multidimensional saddle', *Russ. Math. Surv.* **43**, 264–265.

Turaev, D. & Shil'nikov, L. (1986), 'On bifurcations of homoclinic 'figure eight' from a saddle with a negative saddle value', *Soviet. Math. Dokl.* **34**, 1301–1304.

Yanagida, E. (1987), 'Branching of double pulse solutions from single pulse solutions in nerve axon equations', *J. Diff. Eqs.* **66**, 243–262.